

## Article

# A Dynamic Analysis of Porous Coated Functionally Graded Nanoshells Rested on Viscoelastic Medium

Emad E. Ghandourah <sup>1</sup>, Ahmed Amine Daikh <sup>2,3,\*</sup>, Samir Khatir <sup>4</sup>, Abdulsalam M. Alhawsawi <sup>1</sup>,  
Essam M. Banoqitah <sup>1</sup> and Mohamed A. Eltaher <sup>5</sup>

<sup>1</sup> Nuclear Engineering Department, Center for Training and Radiation Prevention, Faculty of Engineering, King Abdulaziz University, P.O. Box 80204, Jeddah 21589, Saudi Arabia; eghandourah@kau.edu.sa (E.E.G.); amalhawsawi@kau.edu.sa (A.M.A.); ebanoqitah@kau.edu.sa (E.M.B.)

<sup>2</sup> Department of Technology, University Centre of Naama, Naama 45000, Algeria

<sup>3</sup> Laboratoire d'Etude des Structures et de Mécanique des Matériaux, Département de Génie Civil, Faculté des Sciences et de la Technologie, Université Mustapha Stambouli, B.P. 305, Mascara 29000, Algeria

<sup>4</sup> Soete Laboratory, Department of Electrical Energy, Metals, Mechanical Constructions, and Systems, Faculty of Engineering and Architecture, Ghent University, 9000 Gent, Belgium; khatir\_samir@hotmail.fr

<sup>5</sup> Mechanical Engineering Department, Faculty of Engineering, King Abdulaziz University, P.O. Box 80204, Jeddah 21589, Saudi Arabia; meltaher@kau.edu.sa

\* Correspondence: aadaikh@cuniv-naama.dz; Tel.: +213-791064967

**Abstract:** Theoretical research has numerous challenges, particularly about modeling structures, unlike experimental analysis, which explores the mechanical behavior of complex structures. Therefore, this study suggests a new model for functionally graded shell structures called “Tri-coated FGM” using a spatial variation of material properties to investigate the free vibration response incorporating the porosities and microstructure-dependent effects. Two types of tri-coated FG shells are investigated, hardcore and softcore FG shells, and five distribution patterns are proposed. A novel modified field of displacement is proposed by reducing the number of variables from five to four by considering the shear deformation effect. The shell is rested on a viscoelastic Winkler/Pasternak foundation. An analytical solution based on the Galerkin approach is developed to solve the equations of motion derived by applying the principle of Hamilton. The proposed solution is addressed to study different boundary conditions. The current study conducts an extensive parametric analysis to investigate the influence of several factors, including coated FG nanoshell types and distribution patterns, gradient material distribution, porosities, length scale parameter (nonlocal), material scale parameter (gradient), nanoshell geometry, and elastic foundation variation on the fundamental frequencies. The provided results show the accuracy of the developed technique using different boundary conditions.

**Keywords:** coated nanoshells; vibrational behavior; modified four variable HSST; porosity viscoelastic foundation; nonlocal strain gradient theory

**MSC:** 74H45



**Citation:** Ghandourah, E.E.; Daikh, A.A.; Khatir, S.; Alhawsawi, A.M.; Banoqitah, E.M.; Eltaher, M.A. A Dynamic Analysis of Porous Coated Functionally Graded Nanoshells Rested on Viscoelastic Medium. *Mathematics* **2023**, *11*, 2407. <https://doi.org/10.3390/math11102407>

Academic Editors: Subrat Kumar Jena and Dineshkumar Harursampath

Received: 17 April 2023

Revised: 14 May 2023

Accepted: 17 May 2023

Published: 22 May 2023



**Copyright:** © 2023 by the authors. Licensee MDPI, Basel, Switzerland. This article is an open access article distributed under the terms and conditions of the Creative Commons Attribution (CC BY) license (<https://creativecommons.org/licenses/by/4.0/>).

## 1. Introduction

Composite materials are widely merged in various engineering fields, such as aerospace, automobiles, civil engineering, ships, etc., mainly due to their exceptional properties, including light weight, high strength, high modulus, excellent resistance to fatigue, corrosion, etc. However, composites are more easily damaged and delaminated under excessive interlaminar stresses and also are unable to bear high temperatures. As a class of composite materials, functionally graded materials (FGMs) overcome the limitations of traditional composites by comprising two or more different materials with continuity variation from surface to surface. The first FGM was developed by a Japanese scientist in 1984 [1]. The conventional FGMs are formed from metal and ceramic, and the material properties of FGMs are a mixture of the good thermal resistance of ceramics and the high strength and superior

fracture toughness of metals [2]. Since 1984, many researchers have studied the mechanical properties of FGM structures, but most publications considered the material properties in unidirectional FGMs to vary across one direction, from the top to bottom surface [3–6]. Nevertheless, advanced structures in daily life usually are exposed to external loads in more than one direction. To fulfill this demand, it is necessary to develop multi-directional FGMs whose material properties change in different directions, such as the thickness direction and in-plane direction.

Recently, multi-directional FGMs have gained huge attention from the research community, especially regarding their mechanical behavior under vibratory increment. Lu et al. [7] presented a semi-analytical three-directional elasticity study to investigate the deflection and stress responses of multi-directional FGM plates. Nemat-alla [8] developed two-directional FGMs that can reduce the stresses in machine elements under thermal load. Rad [9] established a semi-analytical solution for static analysis of a two-directional FGM circular plate subjected to Winkler–Pasternak elastic foundation bearing transverse and shear loads. Additionally, a semi-analytical solution was proposed by Rad and Alibeligloo [10] to explore the static responses of two-directional FGM circular plates subjected to an elastic foundation. Nazari et al. [11] presented a numerical solution using the first-order shear deformation theory (FSDT) for a geometrically nonlinear dynamic analysis of rectangular plates made of FGM and excited by a moving load. Khakpour et al. [12] determined the natural frequency of functionally graded porous beams. A simply supported boundary condition was provided on elastic substrate in a thermal environment using the third-order shear deformation theory. Tornabene et al. [13] solved the problem of free vibration in sandwich shell structures of FGMs based on developing a numerical model by varying the thickness. Shariyat and Jafari [14] utilized finite element commercial software to study the low-velocity impact of two-directional FGM circular plates under radial preloads. Adineh and Kadkhodayan [15] investigated the deflection and stress responses of a three-directional FGM subjected to an elastic foundation with different boundary conditions. Esmaeilzadeh and Kadkhodayan [16] conducted a dynamic analysis of a two-directional FGM porous plate bearing a moving load. A semi-analytical solution was established by Alipour et al. [17]. The effect of different boundary conditions, material properties and foundations on the frequency responses of the plate was studied. The free vibration of an axially graded beam was investigated by Mikola et al. [18] using the higher order Haar wavelet method (HOHWM) for solutions of both the governing differential equation and the approximation by varying properties of the bending stiffness and the distributed mass per unit length. Using the same technique, Majak et al. [19] studied the vibration behavior of nanobeams for different boundary conditions. Yas and Moloudi [20] presented a semi-analytical solution to explore the free vibration behaviors of multi-directional FGM annular plates with piezo-electric layers. Lieu et al. [21] investigated static bending and dynamic responses of two-directional FGMs by using the isogeometric finite element method. The buckling and dynamic responses of two-directional FGM circular plates bearing hydrostatic in-plane force were assessed by Lal and Ahlawat [22]. Sorrenti et al. [23] provided a review of Haar wavelet methods and developed HOHWM to study the behavior of multilayered composite beams under static and buckling loads. The study employed the refined zigzag theory (RZT) to formulate the corresponding governing differential equations. Majak et al. [24] conducted a study focused on developing accurate and cost-effective function approximation techniques for modeling FGM using HOHWM to expand different grading functions such as exponential and power law into Haar wavelet series. Niknam et al. [25] presented the model of architected multi-directional FGM cellular materials. Based on polyhedral finite elements, Nguyen-Ngoc et al. [26] established a three-dimensional numerical model to explore the static bending and free vibration of multi-directional FGM shells. Asgari and Akhlaghi [27] investigated the free vibration behaviors of two-directional FGM hollow cylinder shells. Zafarmand et al. [28] presented the dynamic responses of two-directional FGM cylindrical shells by using the three-dimensional graded finite element method.

In the literature, researchers have developed several homogenization models to describe the gradation of materials, including the power law model (P-FGM) [29], exponential law model (E-FGM) [30], Sigmoid law model (S-FGM) [31], Tornabene Viola law model [32], trigonometric model [33], Pan exponential law model [34], and cosine trigonometric model [35]. Among these models, the power law is the most commonly cited and accepted in the scientific literature.

In this paper, a new functionally graded model called coated FGM is proposed to further enrich the scientific literature. This model allows for the grading of material properties in all directions, from all surfaces to the core. The provided method can facilitate theoretical studies with greater flexibility for analysis, such as the modeling of gas and wind turbine blades, as presented in Ref. [36]. The free vibration response of coated FG plates/shells incorporating the porosities and microstructure-dependent effects is investigated in this analysis based on a developed Galerkin approach. The proposed solution is limited only to uniform thicknesses and opposite boundary conditions (e.g., SSSS, CCCC, CCSS). The current study is structured as follows: Section 2 provides a detailed explanation of the geometrical modeling and material distribution of the coated functionally graded shells. Section 3 presents the fundamental equations governing the displacements, stress–strain relationship, and equations of motion. Section 4 describes the analytical solution approach based on Galerkin’s method. Section 5 includes the numerical findings and discussions. Finally, Section 6 summarizes the most important outcomes of the study.

## 2. Material Distribution Functions

The dimensions of a rectangular functionally graded shell are presented in Figure 1. The shell is made of aluminum (metal) and alumina (ceramic). Based on the rule of mixture, the effective mechanical properties, such as Young’s modulus  $E$ , Poisson’s ratio  $\nu$ , and density  $\rho$  can be presented as [29]:

$$P(x, y, z) = P_m + (P_c - P_m)V(x, y, z) \quad (1)$$

where  $V(x, y, z)$  represents the spatial variation in the volume fraction of the ceramic phase.  $P_m$  and  $P_c$  represent the mechanical properties of the metal and ceramic, respectively. In the current analysis, two types of ceramic/metal distribution are presented, hardcore (HC) and softcore (SC) FGMs, and the power law functions in three directions are used to define the spatial distribution of materials. Each FGM type has five schemes, FG-A, FG-B, FG-C, FG-D and FG-E, as shown in Figure 2.

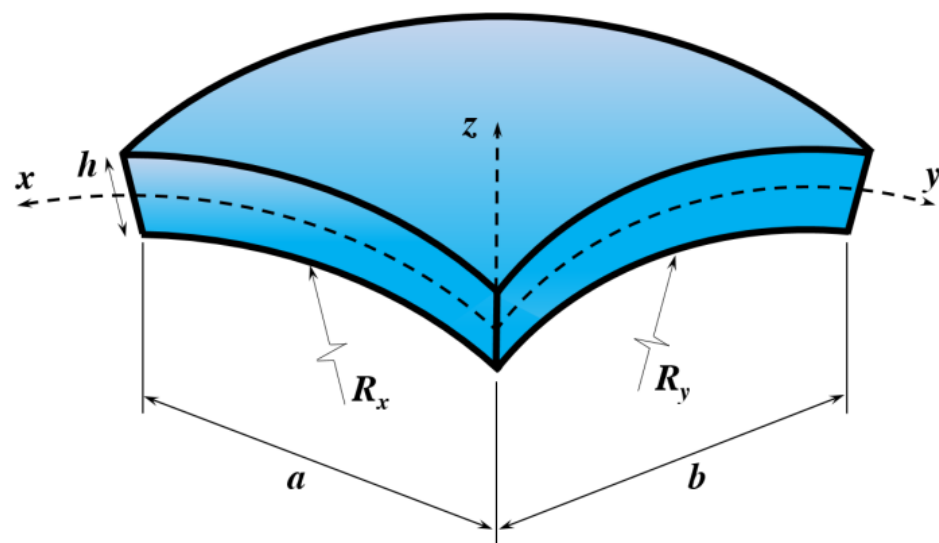


Figure 1. Tri-coated FG spherical shell geometry.

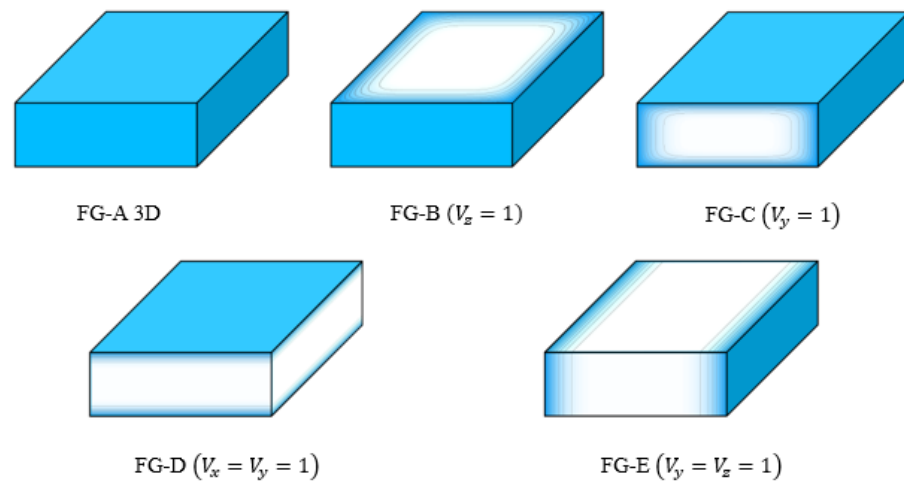


Figure 2. Various schemes of coated FG shell ( $R_x = R_y = \infty$ ).

2.1. Hardcore Coated Functionally Graded Shell (HC)

The volume fraction of the Hardcore shell is provided in the following equation:

$$\begin{cases} V(z) = \left[ \left( \frac{|2z|}{h} \right)^p - 1 \right] + \Lambda_z \\ V(x) = \left[ \left( \frac{|2x-a|}{a} \right)^k - 1 \right] + \Lambda_x \\ V(y) = \left[ \left( \frac{|2y-b|}{b} \right)^e - 1 \right] + \Lambda_y \end{cases} \quad (2)$$

$p, k$  and  $e$  are the power law indexes. The functionally graded material distribution for various power exponents is shown in Figure 3. For the HC-coated functionally graded shell, the total volume fraction can be given as:

$$V(x, y, z) = V(x)V(y)V(z) \quad (3)$$

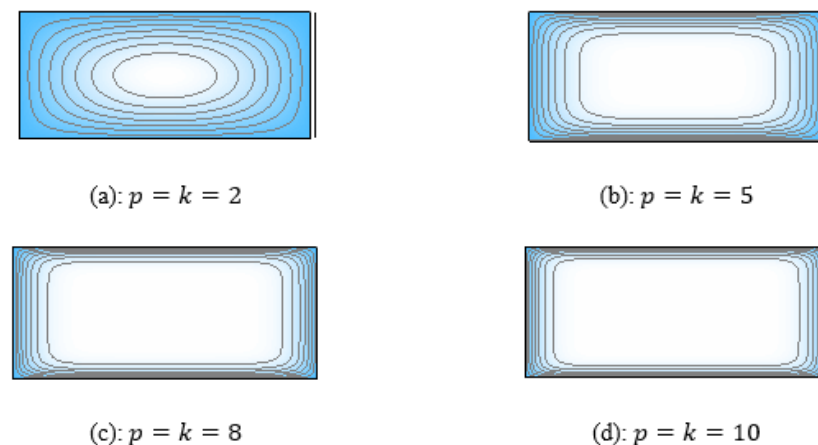


Figure 3. Functionally graded material distribution.

2.2. Softcore Coated Functionally Graded Shell (SC)

The volume fraction of the Softcore shell is provided in the following equation:

$$\begin{cases} V(z) = \left[ \left( \frac{|2z|}{h} \right)^p - 1 \right] - \Lambda_z \\ V(x) = \left[ \left( \frac{|2x-a|}{a} \right)^k - 1 \right] - \Lambda_x \\ V(y) = \left[ \left( \frac{|2y-b|}{b} \right)^e - 1 \right] - \Lambda_y \end{cases} \quad (4)$$

Additionally, the total volume fraction can be given as:

$$V(x, y, z) = 1 - V(x)V(y)V(z) \tag{5}$$

$\Lambda_x, \Lambda_y$  and  $\Lambda_z$  are porosity functions in the  $x, y$  and  $z$  directions, respectively. Four types of porosity distributions are suggested:

- *Even distribution of porosity (Porosity I)*

$$\Lambda_x = \Lambda_y = \Lambda_z = \zeta/2 \tag{6}$$

Here,  $\zeta$  defines the porosity coefficient, where  $0 \leq \zeta \leq 0.2$

- *Uneven distribution of porosity (Porosity II)*

$$\begin{cases} \Lambda_z = \frac{\zeta}{2} \left[ 1 - \frac{2|z|}{h} \right] \\ \Lambda_x = \frac{\zeta}{2} \left[ 1 - \frac{|2x-a|}{a} \right] \\ \Lambda_y = \frac{\zeta}{2} \left[ 1 - \frac{|2y-b|}{b} \right] \end{cases} \tag{7}$$

- *Nonlinear (1) distribution of porosity (Porosity III)*

$$\begin{cases} \Lambda_z = \frac{\zeta}{2} \left[ 1 - \left( 1 + \frac{|2z-1|}{h} \right)^p \right] \\ \Lambda_x = \frac{\zeta}{2} \left[ 1 - \left( \frac{|2x-a|}{a} \right)^k \right] \\ \Lambda_y = \frac{\zeta}{2} \left[ 1 - \left( \frac{|2y-b|}{b} \right)^e \right] \end{cases} \tag{8}$$

- *Nonlinear (2) distribution of porosity (Porosity IV)*

$$\begin{cases} \Lambda_z = \frac{\zeta}{2} \left[ \left( 1 + \frac{|2z-1|}{h} \right)^p \right] \\ \Lambda_x = \frac{\zeta}{2} \left[ \left( \frac{|2x-a|}{a} \right)^k \right] \\ \Lambda_y = \frac{\zeta}{2} \left[ \left( \frac{|2y-b|}{b} \right)^e \right] \end{cases} \tag{9}$$

### 3. Basic Equations

#### 3.1. Generalized Shear Deformation Shell Theory

In the literature, several shell theories were introduced, such as the classical plate theory (CPT), the first-order shear deformation theory (TSDT), and the higher-order shear deformation theory (HSDT). The first-order shear deformation theory was proposed to replace the classical plate theory, in which the effect of transverse shear strain is neglected. Thereafter, to ensure zero shear at the top and bottom surface of the proposed shell, the higher-order shear deformation theory was generated. The displacement field based on the generalized HSDT can be given in the following formulation [37]:

$$\begin{aligned} u(x, y, z, t) &= \left( 1 + \frac{z}{R_x} \right) u_0 - z \frac{\partial w_0}{\partial x} + f(z) \psi_x \\ v(x, y, z, t) &= \left( 1 + \frac{z}{R_y} \right) v_0 - z \frac{\partial w_0}{\partial y} + f(z) \psi_y \\ w(x, y, z, t) &= w_0 \end{aligned} \tag{10}$$

in which  $u, v$  and  $w$  are the displacements in the directions  $x, y$  and  $z$ , respectively.  $\psi_x$  and  $\psi_y$  are the rotations. The shape function for the shear distribution can be given as:

$$f(z) = h \sinh\left(\frac{z}{h}\right) - \frac{3z^3}{2h^2} \tag{11}$$

where  $g(z) = f'(z)$ .

For special cases, when the shell has uniform thickness and the opposite boundary conditions must be the same (e.g., SSSS, CCCC, CCSS), the rotations  $\psi_x$  and  $\psi_y$  take the

same values ( $\psi_x = \psi_y = \psi$ ). Therefore, the field of displacement can be presented in the following formulation:

$$\begin{aligned} u(x, y, z, t) &= \left(1 + \frac{z}{R_x}\right) u_0 - z \frac{\partial w_0}{\partial x} - f(z) \frac{\partial \psi}{\partial x} \\ v(x, y, z, t) &= \left(1 + \frac{z}{R_y}\right) v_0 - z \frac{\partial w_0}{\partial y} - f(z) \frac{\partial \psi}{\partial y} \\ w(x, y, z, t) &= w_0 \end{aligned} \tag{12}$$

where the total number of displacement field unknowns is reduced from five to four unknowns. Based on the assumed modified displacement field described by Equation (12), the strains at any generic point through the domain of the nanoshell can be expressed in the following formulation:

$$\begin{Bmatrix} \varepsilon_{xx} \\ \varepsilon_{yy} \\ \gamma_{xy} \\ \gamma_{yz} \\ \gamma_{xz} \end{Bmatrix} = \begin{bmatrix} u_{0,x} + w_0/R_x & -w_{0,xx} & \psi_{,xx} & 0 & 0 \\ v_{0,y} + w_0/R_y & -w_{0,yy} & \psi_{,yy} & 0 & 0 \\ v_{0,x} + u_{0,y} & -2w_{0,xy} & -2\psi_{,xy} & 0 & 0 \\ 0 & 0 & 0 & \phi_{,y} - \psi_{,y} & 0 \\ 0 & 0 & 0 & \phi_{,x} - \psi_{,x} & 0 \end{bmatrix} \begin{Bmatrix} 1 \\ z \\ f(z) \\ f'(z) \\ f''(z) \end{Bmatrix} \tag{13}$$

Taking into account the action of the strain gradient stress and nonlocal elastic stress, the constitutive equation of the nanoshell can be portrayed as [38]:

$$\sigma_{ij} = \sigma_{ij}^{(0)} - \frac{d\sigma_{ij}^{(1)}}{dx} \tag{14}$$

The stress  $\sigma_{ij}^{(0)}$  and the higher-order stress  $\sigma_{ij}^{(1)}$  are dependent on the strain  $\varepsilon_{kl}$  and the first-order strain gradient  $\varepsilon_{kl,x}$ , and they can be written as

$$\sigma_{ij}^{(0)} = \int_0^L C_{ijkl} \alpha_0(x, x', e_0 a) \varepsilon_{kl}(x') dx' \tag{15}$$

$$\sigma_{ij}^{(1)} = l^2 \int_0^L C_{ijkl} \alpha_1(x, x', e_1 a) \varepsilon_{kl,x}(x') dx' \tag{16}$$

$C_{ijkl}$  are elastic constants,  $l$  represents the material length scale parameter, which describes the field of the strain gradient stress. The nonlocal parameters, which describe the field of the nonlocal elastic stress, are  $e_0 a$  and  $e_1 a$ , and  $\alpha_0(x, x', e_0 a)$  and  $\alpha_1(x, x', e_1 a)$  are the nonlocal kernel functions [39]. The constitutive relation is given as:

$$\left[1 - (e_1 a)^2 \nabla^2\right] \left[1 - (e_0 a)^2 \nabla^2\right] \sigma_{ij} = C_{ijkl} \left[1 - (e_1 a)^2 \nabla^2\right] \varepsilon_{kl} - C_{ijkl} l^2 \left[1 - (e_0 a)^2 \nabla^2\right] \nabla^2 \varepsilon_{kl} \tag{17}$$

$\nabla^2 = \frac{\partial^2}{\partial x^2} + \frac{\partial^2}{\partial y^2}$  describes the Laplacian operator. The nonlocal strain gradient constitutive relations, given in Equation (12) by assuming that  $e = e_0 = e_1$ , can be presented as:

$$\left[1 - \mu \nabla^2\right] \sigma_{ij} = C_{ijkl} \left[1 - \lambda \nabla^2\right] \varepsilon_{kl} \tag{18}$$

where  $\mu = (ea)^2$  and  $\lambda = l^2$ .

The nonlocal strain gradient constitutive stress–strain relations are governed by [40,41]:

$$\begin{Bmatrix} \sigma_{xx} - \mu \nabla^2 \sigma_{xx} \\ \sigma_{yy} - \mu \nabla^2 \sigma_{yy} \\ \tau_{yz} - \mu \nabla^2 \tau_{yz} \\ \tau_{xz} - \mu \nabla^2 \tau_{xz} \\ \tau_{xy} - \mu \nabla^2 \tau_{xy} \end{Bmatrix} = \begin{bmatrix} Q_{11} & Q_{12} & 0 & 0 & 0 \\ Q_{12} & Q_{22} & 0 & 0 & 0 \\ 0 & 0 & Q_{44} & 0 & 0 \\ 0 & 0 & 0 & Q_{55} & 0 \\ 0 & 0 & 0 & 0 & Q_{66} \end{bmatrix} \begin{Bmatrix} \varepsilon_{xx} - \lambda \nabla^2 \varepsilon_{xx} \\ \varepsilon_{yy} - \lambda \nabla^2 \varepsilon_{yy} \\ \gamma_{yz} - \lambda \nabla^2 \gamma_{yz} \\ \gamma_{xz} - \lambda \nabla^2 \gamma_{xz} \\ \gamma_{xy} - \lambda \nabla^2 \gamma_{xy} \end{Bmatrix} \tag{19}$$

where

$$\begin{aligned}
 Q_{11} &= Q_{22} = \frac{E(x,y,z)}{1-\nu^2} \\
 Q_{12} &= \nu Q_{11} \\
 Q_{44} &= Q_{55} = Q_{66} = \frac{E(x,y,z)}{2(1+\nu)}
 \end{aligned}
 \tag{20}$$

Here,  $\nabla^2$  describes the Laplacian operator ( $\nabla^2 = \frac{\partial^2}{\partial x^2} + \frac{\partial^2}{\partial y^2}$ ),  $\mu = (ea)^2$  and  $\lambda = l^2$ . Here,  $ea$  captures the nonlocal effects, while  $l$  captures the strain gradient effects.

### 3.2. Equations of Motion

To obtain the governing equations, the principle of Hamilton is applied, which can be written as:

$$\delta \int_{t_2}^{t_1} \delta(U + F - T)dt = 0
 \tag{21}$$

The variation in the strain energy  $\delta U$  of the coated FG nanoshell is given as:

$$\delta U = \int_V [\sigma_{xx}\delta\epsilon_{xx} + \sigma_{yy}\delta\epsilon_{yy} + \tau_{xy}\gamma_{xy} + \tau_{yz}\gamma_{yz} + \tau_{xz}\gamma_{xz}]dV
 \tag{22}$$

The variation in the kinetic energy  $\delta U$  of the coated FG shell at any moment is expressed as:

$$\delta T = \frac{1}{2} \int_0^L \int_A \rho(\dot{u}\delta\dot{u} + \dot{v}\delta\dot{v} + \dot{w}\delta\dot{w})dAdx
 \tag{23}$$

The Viscoelastic/Winkler/Pasternak foundation is defined as an infinite set of springs, dashpots and viscous elements connected in parallel:

$$\delta F = F_{spring} + F_{shear} + F_{damping} = K_w w(x, y) + K_s \left( \frac{\partial^2 w(x, y)}{\partial x^2} + \frac{\partial^2 w(x, y)}{\partial y^2} \right) + C_d \frac{\partial w(x, y)}{\partial t}
 \tag{24}$$

where  $K_w$ ,  $K_s$  and  $C_d$  are spring, shear and damping parameters of the foundation, respectively.

Inserting Equations (22)–(24) into Equation (21), the equations of motion of the coated FG nanoshells can be obtained as follows:

$$\begin{aligned}
 (1 - \lambda \nabla^2) & \left[ A_{11} \frac{\partial^2 u_0}{\partial x^2} + A_{66} \frac{\partial^2 u_0}{\partial y^2} + (A_{12} + A_{66}) \frac{\partial^2 v_0}{\partial x \partial y} + \left( \frac{A_{11}}{R_x} + \frac{A_{12}}{R_y} \right) \frac{\partial w_0}{\partial x} - B_{11} \frac{\partial^3 w_0}{\partial x^3} \right. \\
 & \left. - (B_{12} + 2B_{66}) \frac{\partial^3 w_0}{\partial x \partial y^2} - C_{11} \frac{\partial^3 \psi}{\partial x^3} - (C_{12} + 2C_{66}) \frac{\partial^3 \psi}{\partial x \partial y^2} \right] \\
 & = (1 - \mu \nabla^2) \left[ \left( I_0 + 2 \frac{I_1}{R_x} + \frac{I_3}{R_y} \right) \frac{\partial^2 u_0}{\partial t^2} - \left( I_1 + \frac{I_2}{R_x} \right) \frac{\partial^3 w_0}{\partial x \partial t^2} - \left( I_3 + \frac{I_4}{R_x} \right) \frac{\partial^2 \psi}{\partial t^2} \right]
 \end{aligned}
 \tag{25}$$

$$\begin{aligned}
 (1 - \lambda \nabla^2) & \left[ (A_{12} + A_{66}) \frac{\partial^2 u_0}{\partial x \partial y} + A_{22} \frac{\partial^2 v_0}{\partial y^2} + A_{66} \frac{\partial^2 v_0}{\partial x^2} - (B_{12} + 2B_{66}) \frac{\partial^3 w_0}{\partial x^2 \partial y} - B_{22} \frac{\partial^3 w_0}{\partial y^3} \right. \\
 & \left. + \left( \frac{A_{12}}{R_x} + \frac{A_{22}}{R_y} \right) \frac{\partial w_0}{\partial x} - (C_{12} + 2C_{66}) \frac{\partial^3 \psi}{\partial x^2 \partial y} - C_{22} \frac{\partial^3 \psi}{\partial y^3} \right] \\
 & = (1 - \mu \nabla^2) \left[ \left( I_0 + 2 \frac{I_1}{R_y} + \frac{I_2}{R_x} \right) \frac{\partial^2 v_0}{\partial t^2} - \left( I_1 + \frac{I_2}{R_y} \right) \frac{\partial^3 w_0}{\partial y \partial t^2} - \left( I_3 + \frac{I_4}{R_y} \right) \frac{\partial^2 \psi}{\partial t^2} \right]
 \end{aligned}
 \tag{26}$$

$$\begin{aligned}
 (1 - \lambda \nabla^2) & \left[ B_{11} \frac{\partial^3 u_0}{\partial x^3} + (B_{12} + 2B_{66}) \frac{\partial^3 u_0}{\partial x \partial y^2} - \left( \frac{A_{11}}{R_x} + \frac{A_{12}}{R_y} \right) \frac{\partial u_0}{\partial x} + (B_{12} + 2B_{66}) \frac{\partial^3 v_0}{\partial x^2 \partial y} + B_{22} \frac{\partial^3 v_0}{\partial y^3} \right. \\
 & - \left( \frac{A_{12}}{R_x} + \frac{A_{22}}{R_y} \right) \frac{\partial v_0}{\partial y} + \left( \frac{2B_{11}}{R_x} + \frac{2B_{12}}{R_y} \right) \frac{\partial^2 w_0}{\partial x^2} - D_{11} \frac{\partial^4 w_0}{\partial x^4} - (2D_{12} + 4D_{66}) \frac{\partial^4 w_0}{\partial x^2 \partial y^2} - D_{22} \frac{\partial^4 w_0}{\partial y^4} \\
 & + \left( \frac{2B_{12}}{R_x} + \frac{2B_{22}}{R_y} \right) \frac{\partial^2 w_0}{\partial y^2} - \left( \frac{A_{11}}{R_x} + 2 \frac{A_{12}}{R_x R_y} + \frac{A_{22}}{R_y} \right) w_0 - E_{11} \frac{\partial^4 \psi}{\partial x^4} - 2(E_{12} + 2E_{66}) \frac{\partial^4 \psi}{\partial x^2 \partial y^2} \\
 & - E_{22} \frac{\partial^4 \psi}{\partial y^4} + \left( \frac{C_{11}}{R_x} + \frac{C_{12}}{R_y} \right) \frac{\partial^2 \psi}{\partial x^2} + \left( \frac{C_{12}}{R_x} + \frac{C_{22}}{R_y} \right) \frac{\partial^2 \psi}{\partial y^2} \Big] = (1 - \mu \nabla^2) \left[ I_0 \frac{\partial^2 w_0}{\partial t^2} \right. \\
 & \left. + \left( I_1 + \frac{I_2}{R_x} \right) \frac{\partial^3 u_0}{\partial x \partial t^2} + \left( I_1 + \frac{I_2}{R_y} \right) \frac{\partial^3 v_0}{\partial y \partial t^2} - I_2 \left( \frac{\partial^4 w_0}{\partial x^2 \partial t^2} + \frac{\partial^4 w_0}{\partial y^2 \partial t^2} \right) + I_4 \left( \frac{\partial^3 \psi}{\partial x \partial t^2} + \frac{\partial^3 \psi}{\partial y \partial t^2} \right) \right]
 \end{aligned}
 \tag{27}$$

$$\begin{aligned}
 & (1 - \lambda \nabla^2) \left[ \begin{aligned} & C_{11} \frac{\partial^3 u}{\partial x^3} + (C_{12} + 2C_{66}) \frac{\partial^3 u}{\partial x \partial y^2} + (C_{12} + 2C_{66}) \frac{\partial^3 v}{\partial x^2 \partial y} + C_{22} \frac{\partial^3 v}{\partial y^3} - E_{11} \frac{\partial^4 w_0}{\partial x^4} \\ & - 2(E_{12} + 2E_{66}) \frac{\partial^4 w_0}{\partial x^2 \partial y^2} - E_{22} \frac{\partial^4 w_0}{\partial x^4} - F_{11} \frac{\partial^4 \psi}{\partial x^4} - 2(F_{12} + 2F_{66}) \frac{\partial^4 \psi}{\partial x^2 \partial y^2} \\ & - F_{22} \frac{\partial^4 \psi}{\partial y^4} + J_{44} \frac{\partial^2 \psi}{\partial y^2} + J_{55} \frac{\partial^2 \psi}{\partial x^2} + \left( \frac{C_{11}}{R_x} + \frac{C_{12}}{R_y} \right) \frac{\partial^2 w}{\partial x^2} + \left( \frac{C_{12}}{R_x} + \frac{C_{22}}{R_y} \right) \frac{\partial^2 w}{\partial y^2} \end{aligned} \right] \\
 = & (1 - \mu \nabla^2) \left[ \left( I_3 + \frac{I_4}{R_x} \right) \left( \frac{\partial^3 u_0}{\partial x \partial t^2} + \frac{\partial^3 v_0}{\partial y \partial t^2} \right) - I_4 \left( \frac{\partial^4 w_0}{\partial x^2 \partial t^2} + \frac{\partial^4 w_0}{\partial y^2 \partial t^2} \right) - I_5 \left( \frac{\partial^4 \psi}{\partial x^2 \partial t^2} + \frac{\partial^4 \psi}{\partial y^2 \partial t^2} \right) \right]
 \end{aligned} \tag{28}$$

The coefficients of the stiffness can be expressed as:

$$\begin{aligned}
 \{A_{ij}, B_{ij}, D_{ij}, C_{ij}, F_{ij}, H_{ij}\} &= \int Q_{ij} \{1, z, z^2, f(z), zf(z), f(z)^2\} dx dy dz, \quad (i, j = 1, 2, 6) \\
 J_{ii} &= \int Q_{ii} (f'(z))^2 dx dy dz, \quad (i = 4, 5)
 \end{aligned} \tag{29}$$

and

$$\{I_0, I_1, I_2, I_3, I_4, I_5\} = \rho(x, y, z) \{1, z, z^2, f(z), zf(z), (\Phi(z))^2\} dx dy dz \tag{30}$$

### 4. Analytical Solution

By considering the four unknowns of displacements and examining various boundary conditions, the Galerkin approach is employed. Galerkin expressions of displacements can be provided as [42–44]:

$$\begin{aligned}
 u_0 &= \sum_{m=1}^{\infty} \sum_{n=1}^{\infty} U_{mn} \cdot \frac{\partial X_m(x)}{\partial x} Y_n(y) e^{i\omega t} \\
 v_0 &= \sum_{m=1}^{\infty} \sum_{n=1}^{\infty} V_{mn} \cdot X_m(x) \frac{\partial Y_n(y)}{\partial y} e^{i\omega t} \\
 \{w_0, \psi\} &= \sum_{m=1}^{\infty} \sum_{n=1}^{\infty} \{W_{mn}, \Psi_{mn}\} X_m(x) Y_n(y) e^{i\omega t}
 \end{aligned} \tag{31}$$

The arbitrary parameters are defined as  $U_{mn}, V_{mn}, W_{mn}, \Psi_{mn}$  and  $\Phi_{mn}$ .  $m$  and  $n$  are mode numbers, and  $\omega$  represents the natural frequency. The functions  $X_m(x)$  and  $Y_n(y)$  that satisfy the simply supported and/or clamped boundary conditions are represented in Table 1 and Figure 4.

**Table 1.** The admissible functions  $X_m(x)$  and  $Y_n(y)$  for different boundary conditions [35].

	Boundary Conditions		The Functions $X_m$ and $Y_n$	
	At $x = 0, a$	At $y = 0, b$	$X_m(x)$	$Y_n(y)$
SSSS	$X_m(0) = X_m''(0) = 0$ $X_m(a) = X_m''(a) = 0$	$Y_n(0) = Y_n''(0) = 0$ $Y_n(b) = Y_n''(b) = 0$	$\sin(\alpha x)$	$\sin(\beta y)$
CCCC	$X_m(0) = X_m'(0) = 0$ $X_m(a) = X_m'(a) = 0$	$Y_n(0) = Y_n'(0) = 0$ $Y_n(b) = Y_n'(b) = 0$	$\sin^2(\alpha x)$	$\sin^2(\beta y)$
CCSS	$X_m(0) = X_m'(0) = 0$ $X_m(a) = X_m''(a) = 0$	$Y_n(0) = Y_n'(0) = 0$ $Y_n(b) = Y_n''(b) = 0$	$\sin(\alpha x)[\cos(\alpha x) - 1]$	$\sin(\beta y)[\cos(\beta y) - 1]$

where  $\alpha = m\pi/a, \beta = n\pi/b$ .

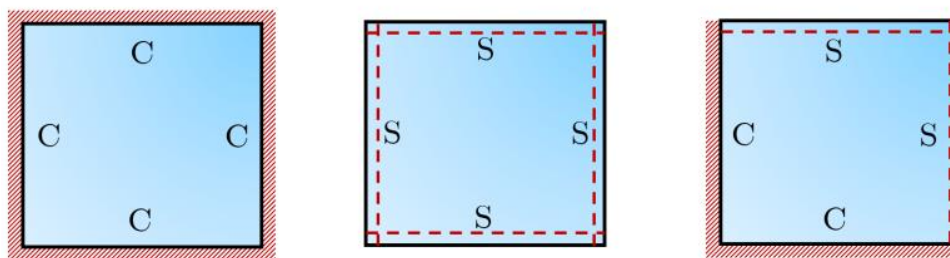


**Figure 4.** Different boundary conditions of the nanoshell.

Inserting Equation (31) into Equations (25)–(28), one obtains

$$[K] - \omega_{mn}^2 [M] = 0 \tag{32}$$

[K] and [M] are the rigidity matrix and mass matrix represented in Appendix A.

### 5. Results and Discussion

A rectangular FG nanoshell of thickness, length and width  $h \times a \times b$ , made of a mixture of aluminum and alumina (Al/Al<sub>2</sub>O<sub>3</sub>) with the following material properties:

$$\begin{aligned} \text{Aluminum Al : } E_m &= 70 \text{ GPa, } \rho_m = 2707 \text{ Kg/m}^3 \text{ } v_m = 0.3 \\ \text{Alumina Al}_2\text{O}_3 : E_c &= 380 \text{ GPa, } \rho_c = 3800 \text{ Kg/m}^3 \text{ } v_c = 0.3 \end{aligned}$$

The dimensionless values of frequency and various foundation parameters are given as:

$$\bar{\omega} = 10^2 \omega h \sqrt{\frac{\rho_c}{E_c}} \tag{33}$$

$$K_w = \frac{k_w a^2}{D}, \quad K_s = \frac{k_s}{D}, \quad C_d = c_d (hD\rho_c)^{-1} \tag{34}$$

where  $D = \frac{E_c h^3}{12(1-\nu^2)}$ .

Table 2 presents a comparative analysis aimed at validating the accuracy of the current approach for computing the dimensionless frequencies  $\tilde{\omega}$  of simply supported square Al/Al<sub>2</sub>O<sub>3</sub> FG plates and doubly curved shells using the proposed specific solution. The results demonstrate that the difference between the proposed method and the previously published data is minimal, indicating that the proposed model is precise and effective for analyzing the mechanical behavior of FG shells.

**Table 2.** Comparison of natural frequency parameter ( $\tilde{\omega} = \omega h \sqrt{\rho_c/E_c}$ ) for simply supported Al/Al<sub>2</sub>O<sub>3</sub> functionally graded shells ( $b = a = 10h$ ).

$a/R_x$	$b/R_y$	$p$	Present	Ref. [45]	Error. (%)	Ref. [37]	Error. (%)	Ref. [46]	Error. (%)	Ref. [47]	Error. (%)
0.5	0.5	0	0.0753	0.0779	0.08	0.0751	0.08	0.0762	0.08	0.0761	1.05
		0.5	0.0653	0.0676	0.07	0.0657	0.07	0.0664	0.07	0.0662	1.36
		1	0.0595	0.0617	0.06	0.0601	0.06	0.0607	0.06	0.0605	1.65
		4	0.0496	0.0519	0.05	0.0503	0.05	0.0509	0.05	0.0506	1.98
		10	0.0459	0.0482	0.05	0.0464	0.05	0.0471	0.05	0.0467	1.71
0.5	0	0	0.0622	0.0648	0.06	0.0622	0.06	0.0629	0.06	0.0628	0.96
		0.5	0.0533	0.0553	0.06	0.0535	0.05	0.0540	0.05	0.0538	0.93
		1	0.0482	0.0501	0.05	0.0485	0.05	0.0490	0.05	0.0488	1.23
		4	0.0410	0.0430	0.04	0.0413	0.04	0.0419	0.04	0.0416	1.44
		10	0.0387	0.0408	0.04	0.0390	0.04	0.0395	0.04	0.0392	1.28
0.5	-0.5	0	0.0563	0.0597	0.06	0.0563	0.06	0.0580	0.06	0.0577	2.43
		0.5	0.0478	0.0506	0.05	0.0479	0.05	0.0493	0.05	0.0490	2.45
		1	0.0431	0.0456	0.05	0.0432	0.04	0.0445	0.04	0.0442	2.49
		4	0.0371	0.0396	0.04	0.0372	0.04	0.0385	0.04	0.0381	2.62
		10	0.0354	0.0380	0.04	0.0355	0.04	0.0368	0.04	0.0364	2.75

$$\text{Error} = |(\hat{w}_{\text{Present}} - \hat{w}_{\text{Ref}}) / \hat{w}_{\text{Ref}}| \times 100\%.$$

Table 3 examines the impact of the variation in the inhomogeneity parameters  $p, k$ , and  $e$  on the dimensionless frequency  $\bar{\omega}$  of coated FG spherical shells ( $R_x/a = R_y/b = 5$ ). Various schemes and types of FG coated shells are investigated. The vibrational behavior of the same structures is analyzed in Table 4 by changing the radius of curvature.

**Table 3.** Dimensionless frequency  $\bar{\omega}$  of coated FGM shells versus exponents  $p$ ,  $k$  and  $e$  (SSSS,  $R_x/a = R_y/b = 5$ ,  $b = a = 10h$ ,  $\mu = \lambda = C_t = K_w = K_s = 0$ ).

$p$	$k$	$e$	Hardcore					Softcore				
			FG-A	FG-B	FG-C	FG-D	FG-E	FG-A	FG-B	FG-C	FG-D	FG-E
2	2	2	4.0055	4.9170	4.3295	4.7239	5.4687	5.8258	5.2103	5.6590	5.3289	4.5795
		5	4.1749	5.2103	4.3295	4.7239	5.4687	5.7460	4.9170	5.6590	5.3289	4.5795
		10	4.2468	5.3316	4.3295	4.7239	5.4687	5.7074	4.7697	5.6590	5.3289	4.5795
	5	2	4.1749	5.2103	4.5382	4.7239	5.8052	5.7460	4.9170	5.5106	5.3289	3.9571
		5	4.3661	5.5287	4.5382	4.7239	5.8052	5.6359	4.4867	5.5106	5.3289	3.9571
		10	4.4465	5.6590	4.5382	4.7239	5.8052	5.5812	4.2608	5.5106	5.3289	3.9571
	10	2	4.2468	5.3316	4.6252	4.7239	5.9414	5.7074	4.7697	5.4334	5.3289	3.6077
		5	4.4465	5.6590	4.6252	4.7239	5.9414	5.5812	4.2608	5.4334	5.3289	3.6077
		10	4.5300	5.7923	4.6252	4.7239	5.9414	5.5173	3.9864	5.4334	5.3289	3.6077
5	2	2	4.3796	4.9170	4.8036	5.3009	5.4687	5.6187	5.2103	5.3107	4.6802	4.5795
		5	4.6032	5.2103	4.8036	5.3009	5.4687	5.4723	4.9170	5.3107	4.6802	4.5795
		10	4.6969	5.3316	4.8036	5.3009	5.4687	5.4009	4.7697	5.3107	4.6802	4.5795
	5	2	4.6032	5.2103	5.0692	5.3009	5.8052	5.4723	4.9170	5.0308	4.6802	3.9571
		5	4.8506	5.5287	5.0692	5.3009	5.8052	5.2675	4.4867	5.0308	4.6802	3.9571
		10	4.9532	5.6590	5.0692	5.3009	5.8052	5.1645	4.2608	5.0308	4.6802	3.9571
	10	2	4.6969	5.3316	5.1783	5.3009	5.9414	5.4009	4.7697	4.8832	4.6802	3.6077
		5	4.9532	5.6590	5.1783	5.3009	5.9414	5.1645	4.2608	4.8832	4.6802	3.6077
		10	5.0590	5.7923	5.1783	5.3009	5.9414	5.0434	3.9864	4.8832	4.6802	3.6077
10	2	2	4.5963	4.9170	5.0737	5.6245	5.4687	5.4711	5.2103	5.0548	4.1843	4.5795
		5	4.8489	5.2103	5.0737	5.6245	5.4687	5.2745	4.9170	5.0548	4.1843	4.5795
		10	4.9542	5.3316	5.0737	5.6245	5.4687	5.1778	4.7697	5.0548	4.1843	4.5795
	5	2	4.8489	5.2103	5.3690	5.6245	5.8052	5.2745	4.9170	4.6694	4.1843	3.9571
		5	5.1261	5.5287	5.3690	5.6245	5.8052	4.9957	4.4867	4.6694	4.1843	3.9571
		10	5.2403	5.6590	5.3690	5.6245	5.8052	4.8542	4.2608	4.6694	4.1843	3.9571
	10	2	4.9542	5.3316	5.4895	5.6245	5.9414	5.1778	4.7697	4.4647	4.1843	3.6077
		5	5.2403	5.6590	5.4895	5.6245	5.9414	4.8542	4.2608	4.4647	4.1843	3.6077
		10	5.3577	5.7923	5.4895	5.6245	5.9414	4.6870	3.9864	4.4647	4.1843	3.6077

**Table 4.** Dimensionless frequency  $\bar{\omega}$  of coated FGM shells with various geometries (SSSS,  $b = a = 10h$ ,  $\mu = \lambda = C_t = K_w = K_s = 0$ ).

$\frac{R_x}{a} \cdot \frac{R_y}{b}$	$p.k.e$	Hardcore					Softcore				
		FG-A	FG-B	FG-C	FG-D	FG-E	FG-A	FG-B	FG-C	FG-D	FG-E
5. 5	2	4.0055	4.9170	4.3295	4.7239	5.4687	5.8258	5.2103	5.6590	5.3289	4.5795
	5	4.8506	5.5287	5.0692	5.3009	5.8052	5.2675	4.4867	5.0308	4.6802	3.9571
	10	5.3577	5.7923	5.4895	5.6245	5.9414	4.6870	3.9864	4.4647	4.1843	3.6077
5. -5	2	3.7255	4.6385	4.0137	4.3656	5.1589	5.5258	4.9151	5.3862	5.1039	4.3201
	5	4.5271	5.2155	4.7281	4.9411	5.4762	5.0135	4.2326	4.8028	4.4887	3.7331
	10	5.0209	5.4641	5.1436	5.2692	5.6047	4.4643	3.7608	4.2620	4.0067	3.4036
5. inf	2	3.8048	4.7190	4.1029	4.4665	5.2485	5.6136	5.0005	5.4666	5.1716	4.3951
	5	4.6192	5.3061	4.8251	5.0434	5.5714	5.0884	4.3061	4.8706	4.5466	3.7979
	10	5.1173	5.5590	5.2426	5.3708	5.7021	4.5301	3.8260	4.3223	4.0601	3.4627

The influence of porosity types on the vibration response of coated FG spherical shells with simply supported ends is illustrated in Table 5. The porosity coefficient is taken as 0.1, 0.2. It is seen that the porosities have a significant influence on the response.

**Table 5.** Dimensionless frequency  $\bar{\omega}$  of porous coated FGM shells ( $p = k = e = 2$ ,  $SSSS$ ,  $R_x/a = R_y/b = 5$ ,  $b = a = 10h$ ,  $\mu = \lambda = C_t = K_w = K_s = 0$ ).

Type of Porosity	$\xi$	Hardcore					Softcore				
		FG-A	FG-B	FG-C	FG-D	FG-E	FG-A	FG-B	FG-C	FG-D	FG-E
I	0.1	3.8451	4.7723	4.1594	4.5901	5.3592	5.7250	5.0323	5.5359	5.1857	4.4096
	0.2	3.6982	4.5961	4.0124	4.4722	5.2499	5.5962	4.8241	5.3896	5.0288	4.2263
II	0.1	3.9311	4.8628	4.2688	4.6916	5.4132	5.7919	5.1247	5.6201	5.2854	4.4961
	0.2	3.8589	4.7675	4.2079	4.6587	5.3563	5.7542	5.0323	5.5775	5.2373	4.4096
III	0.1	3.9207	4.8310	4.2407	4.6703	5.3944	5.7762	5.0947	5.6011	5.2637	4.4676
	0.2	3.8215	4.7039	4.1521	4.6150	5.3174	5.7187	4.9666	5.5361	5.1907	4.3501
IV	0.1	3.9446	4.8990	4.2469	4.6451	5.4346	5.7808	5.1539	5.5989	5.2524	4.5242
	0.2	3.8825	4.8486	4.1826	4.5842	5.4049	5.7315	5.0947	5.5349	5.1738	4.4676

Dimensionless frequency  $\bar{\omega}$  of simply supported coated FG nanoshells influenced by the nonlocal and length-scale parameters is tabulated in Table 6 by considering various distribution patterns. From this table, the stiffness of the nanoshell is affected by the length-scale and the nonlocal parameters, where the augmentation of the nonlocal parameter  $\mu$  leads to a diminishing in the frequencies because of the reduction in the rigidity of the nanoshell. The inverse impact is detected by the increase in the length-scale parameter where the rigidity augments. For the hardcore shell, the highest and lowest natural frequencies are obtained for FG-E and FG-A, respectively. However, the inverse observation is noticed for the softcore arrangement.

**Table 6.** Dimensionless frequency  $\bar{\omega}$  of coated FGM nanoshells versus nonlocal and length-scale parameters ( $SSSS$ ,  $p = 2$ ,  $R_x/a = R_y/b = 5$ ,  $b = a = 10h$ ,  $C_t = K_w = K_s = 0$ ).

$\mu$	$\lambda$	Hardcore					Softcore				
		FG-A	FG-B	FG-C	FG-D	FG-E	FG-A	FG-B	FG-C	FG-D	FG-E
0	0	4.0055	4.9170	4.3295	4.7239	5.4687	5.8258	5.2103	5.6590	5.3289	4.5795
	0.5	4.2163	5.1720	4.5582	4.9744	5.7524	6.1262	5.4805	5.9496	5.6006	4.8169
	1	4.4105	5.4084	4.7686	5.2044	6.0155	6.4054	5.7311	6.2202	5.8543	5.0370
	1.5	4.5915	5.6300	4.9645	5.4184	6.2620	6.6677	5.9659	6.4748	6.0935	5.2434
	2	4.7620	5.8395	5.1488	5.6195	6.4951	6.9161	6.1880	6.7160	6.3207	5.4384
0.5	0	3.8217	4.6912	4.1308	4.5070	5.2176	5.5582	4.9710	5.3991	5.0842	4.3693
	0.5	4.0228	4.9345	4.3490	4.7460	5.4882	5.8448	5.2288	5.6763	5.3434	4.5958
	1	4.2081	5.1600	4.5497	4.9654	5.7392	6.1112	5.4679	5.9345	5.5854	4.8058
	1.5	4.3808	5.3714	4.7366	5.1696	5.9744	6.3614	5.6919	6.1773	5.8137	5.0026
	2	4.5434	5.5713	4.9124	5.3614	6.1967	6.5983	5.9037	6.4075	6.0304	5.1887
1	0	3.6612	4.4940	3.9572	4.3175	4.9981	5.3244	4.7620	5.1720	4.8704	4.1856
	0.5	3.8538	4.7270	4.1662	4.5464	5.2574	5.5989	5.0089	5.4376	5.1187	4.4026
	1	4.0312	4.9430	4.3584	4.7566	5.4977	5.8541	5.2379	5.6849	5.3505	4.6037
	1.5	4.1967	5.1455	4.5375	4.9522	5.7230	6.0938	5.4525	5.9175	5.5691	4.7923
	2	4.3524	5.3370	4.7058	5.1359	5.9360	6.3207	5.6554	6.1379	5.7767	4.9705
1.5	0	3.5194	4.3198	3.8038	4.1501	4.8043	5.1179	4.5773	4.9714	4.6816	4.0234
	0.5	3.7045	4.5437	4.0047	4.3701	5.0535	5.3817	4.8147	5.2267	4.9202	4.2319
	1	3.8750	4.7514	4.1895	4.5722	5.2845	5.6270	5.0347	5.4644	5.1430	4.4253
	1.5	4.0340	4.9460	4.3615	4.7601	5.5010	5.8574	5.2410	5.6879	5.3531	4.6065
	2	4.1837	5.1300	4.5234	4.9367	5.7057	6.0755	5.4360	5.8998	5.5527	4.7778
2	0	3.3929	4.1644	3.6671	4.0008	4.6314	4.9337	4.4126	4.7925	4.5132	3.8787
	0.5	3.5714	4.3803	3.8607	4.2129	4.8716	5.1880	4.6414	5.0386	4.7431	4.0797
	1	3.7357	4.5804	4.0388	4.4077	5.0943	5.4244	4.8536	5.2677	4.9579	4.2661
	1.5	3.8890	4.7680	4.2047	4.5888	5.3030	5.6465	5.0524	5.4832	5.1605	4.4408
	2	4.0333	4.9453	4.3607	4.7591	5.5003	5.8568	5.2403	5.6874	5.3528	4.6059

In Table 7, the dimensionless frequency  $\bar{\omega}$  of coated FG shells versus the aspect ratio is tabulated for various boundary conditions. It is worth mentioning that the highest frequencies are obtained for the fully clamped shells, whereas the lowest frequencies are for the simply supported ones.

**Table 7.** Dimensionless frequency  $\bar{\omega}$  of coated FGM shells versus the aspect ratio ( $R_x/a = R_y/b = 5, a = 10h, \mu = \lambda = C_t = K_w = K_s = 0$ ).

BCs.	$bla$	Hardcore					Softcore				
		FG-A	FG-B	FG-C	FG-D	FG-E	FG-A	FG-B	FG-C	FG-D	FG-E
SSSS	0.5	9.1619	11.2542	9.8934	10.7837	12.5161	13.2973	11.9250	12.8725	11.9495	10.4823
	1	4.0055	4.9170	4.3295	4.7239	5.4687	5.8258	5.2103	5.6590	5.3289	4.5795
	2	2.5101	3.0935	2.7117	2.9573	3.4410	3.6743	3.2782	3.5761	3.3879	2.8809
	3	2.1746	2.6964	2.3463	2.5557	2.9994	3.2109	2.8575	3.1304	2.9765	2.5111
CCCC	0.5	17.1757	20.5725	18.6212	20.3661	22.8825	23.9064	21.8004	22.8049	20.2667	19.1594
	1	7.1130	8.6916	7.6910	8.3931	9.6678	10.2469	9.2105	9.9013	9.1508	8.0944
	2	4.9556	6.0692	5.3577	5.8464	6.7512	7.1709	6.4317	6.9435	6.4631	5.6520
	3	4.6526	5.7008	5.0296	5.4878	6.3415	6.7371	6.0414	6.5243	6.0743	5.3089
CSCS	0.5	16.1992	19.6201	17.5320	19.1469	21.8226	22.9562	20.7909	22.0272	19.9015	18.2729
	1	6.8300	8.3911	7.3782	8.0451	9.3334	9.9241	8.8920	9.6157	8.9589	7.8147
	2	4.5431	5.5965	4.9068	5.3495	6.2253	6.6350	5.9308	6.4431	6.0494	5.2118
	3	4.1493	5.1173	4.4806	4.8840	5.6924	6.0707	5.4230	5.8980	5.5450	4.7655

In order to examine the vibrational behavior of the tri-coated FG shells resting on a Winkler/Pasternak viscoelastic foundation, a parametric study is performed by varying the various foundation parameters such as the Winkler foundation parameter  $K_w$ , the Pasternak foundation parameters  $K_s$  and the damping coefficient  $C_d$ . Table 8 illustrates the influence of the mentioned parameters on dimensional frequencies.

**Table 8.** Dimensionless frequency  $\bar{\omega}$  of coated FGM shells versus elastic foundation parameters (SSSS,  $p = 2R_x/a = R_y/b = 5, b = a = 10h, \mu = \lambda = 0$ ).

$C_d$	$K_w$	$K_s$	Hardcore					Softcore				
			FG-A	FG-B	FG-C	FG-D	FG-E	FG-A	FG-B	FG-C	FG-D	FG-E
0	0	0	4.0055	4.9170	4.3295	4.7239	5.4687	5.8258	5.2103	5.6590	5.3289	4.5795
		50	8.4668	8.7744	8.4604	8.4517	8.8876	9.0797	8.8333	9.1046	9.1277	8.7104
		100	11.2829	11.3923	11.1533	10.9789	11.3163	11.4424	11.3530	11.5649	11.7561	11.4345
	50	0	4.6565	5.4340	4.9090	5.2242	5.9060	6.2333	5.6835	6.0974	5.8277	5.1512
		50	8.7934	9.0742	8.7710	8.7411	9.1630	9.3463	9.1204	9.3833	9.4275	9.0240
		100	11.5299	11.6247	11.3906	11.2031	11.5338	11.6551	11.5777	11.7855	11.9903	11.6751
	100	0	5.2270	5.9059	5.4270	5.6806	6.3130	6.6158	6.1203	6.5064	6.2871	5.6655
		50	9.1082	9.3643	9.0710	9.0212	9.4305	9.6056	9.3987	9.6540	9.7180	9.3271
		100	11.7717	11.8525	11.6231	11.4230	11.7474	11.8639	11.7982	12.0021	12.2199	11.9107
10	0	2	3.5457	4.5879	3.9515	4.4283	5.216	5.5949	4.9239	5.3966	5.0016	4.1943
		5	8.2596	8.5946	8.2736	8.2903	8.7345	8.9334	8.6676	8.9440	8.9409	8.5146
		10	11.1290	11.255	11.0120	10.8550	11.1970	11.3270	11.2250	11.4390	11.6120	11.2860
	50	2	4.2675	5.1382	4.5792	4.9586	5.6728	6.0181	5.4222	5.8548	5.5301	4.8121
		5	8.5941	8.9004	8.5910	8.5852	9.0146	9.2043	8.9600	9.2276	9.2468	8.8351
		10	11.3790	11.4900	11.2530	11.0820	11.4160	11.5420	11.4520	11.6620	11.8490	11.5300
	100	2	4.8837	5.6350	5.1306	5.4373	6.0954	6.4135	5.8785	6.2796	6.0123	5.3591
		5	8.9160	9.1961	8.8971	8.8703	9.2864	9.4675	9.2432	9.5028	9.5429	9.1445
		10	11.6240	11.7200	11.488	11.3040	11.6320	11.7530	11.6750	11.8810	12.0810	11.7690

Table 8. Cont.

$C_d$	$K_w$	$K_s$	Hardcore					Softcore				
			FG-A	FG-B	FG-C	FG-D	FG-E	FG-A	FG-B	FG-C	FG-D	FG-E
20	0	2	1.467	3.4153	2.4944	3.3904	4.3707	4.8364	3.9415	4.5186	3.8558	2.7294
		5	7.6038	8.0309	7.6858	7.7860	8.2580	8.4795	8.1504	8.4440	8.3552	7.8975
		10	10.652	10.8310	10.5790	10.4760	10.8290	10.9730	10.8310	11.0530	11.1680	10.8290
	50	2	2.7916	4.1253	3.4026	4.0586	4.9069	5.3203	4.5489	5.0571	4.5205	3.6076
		5	7.966	8.3574	8.0266	8.0993	8.5539	8.7645	8.4607	8.7439	8.6819	8.2423
		10	10.913	11.075	10.829	10.71	11.0570	11.194	11.066	11.284	11.4150	11.0830
	100	2	3.6652	4.7298	4.1149	4.6315	5.3900	5.7638	5.0843	5.5435	5.0993	4.3105
		5	8.3124	8.6717	8.3534	8.4009	8.8398	9.0405	8.7601	9.0339	8.9967	8.5731
		10	11.169	11.3140	11.0730	10.9400	11.279	11.4120	11.2970	11.5100	11.6560	11.3310

To understand more the impact of various material and geometrical parameters on the frequencies of uni-, bi- and tri-coated FG shells using the proposed specific solution, Figures 5–16 are plotted. Dimensionless frequencies of various schemes of FG shell in the function of material distribution indexes  $p$ ,  $k$  and  $e$  are shown in Figure 5. The inhomogeneity indexes are varied from 0 to 10. In the case of the hardcore FG structure, and for all FG schemes, the augmentation in the indexes  $p$ ,  $k$  and  $e$  leads to an improvement in the shell stiffness, and, therefore, an increment in the dimensionless frequencies. For the softcore FG structure, the inverse action of the inhomogeneity indexes  $p$ ,  $k$  and  $e$  on the shell stiffness is obtained, where the dimensionless frequencies are reduced by the increase in the inhomogeneity indexes. The case of  $p = k = e = 0$  means that the shell is fully metal for the hardcore structure and fully ceramic for the softcore structure. To further clarify, the action of exponents  $p$  and  $k$  on the dimensionless frequency of simply supported hardcore/softcore FG-C coated shells is presented in Figure 6.

The impact of the geometric parameter “ $b/a$ ” on the dimensionless frequencies of various types of the coated shell with simply supported boundary conditions is examined in Figure 7. Regardless of the FG coated shell types and schemes, it is seen that the increase in the parameter “ $b/a$ ” makes the FG shell softer, and this leads to a reduction in the dimensionless frequencies.

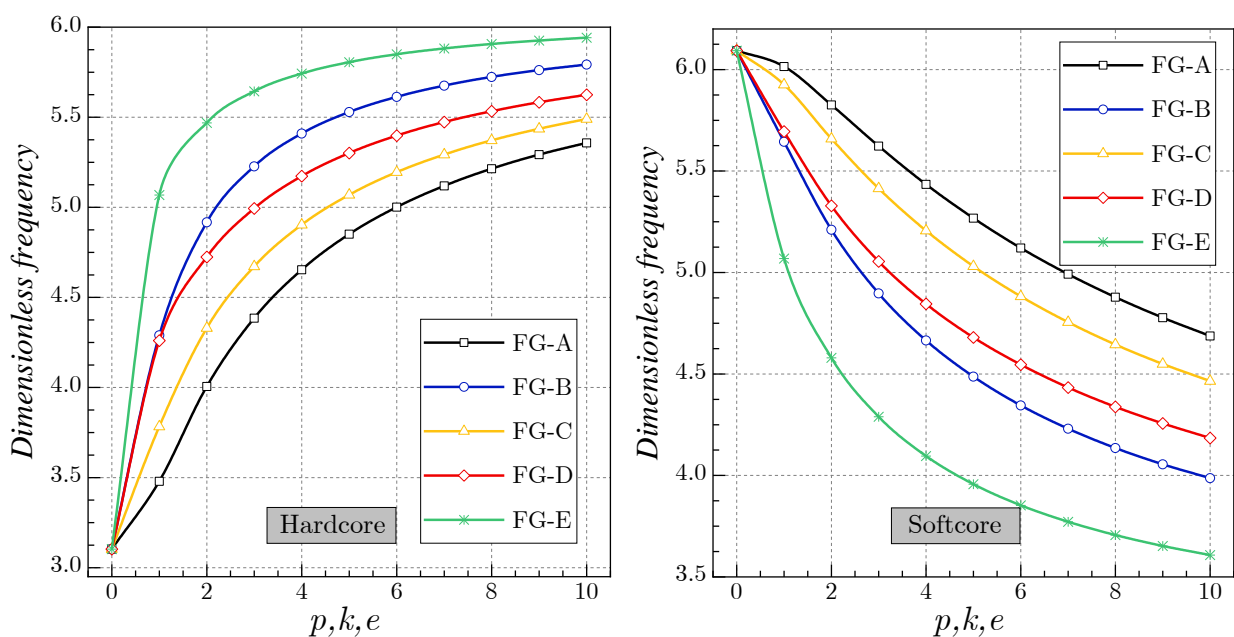
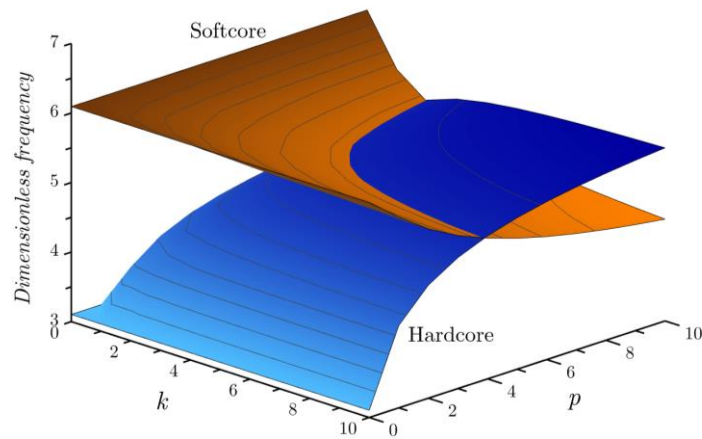
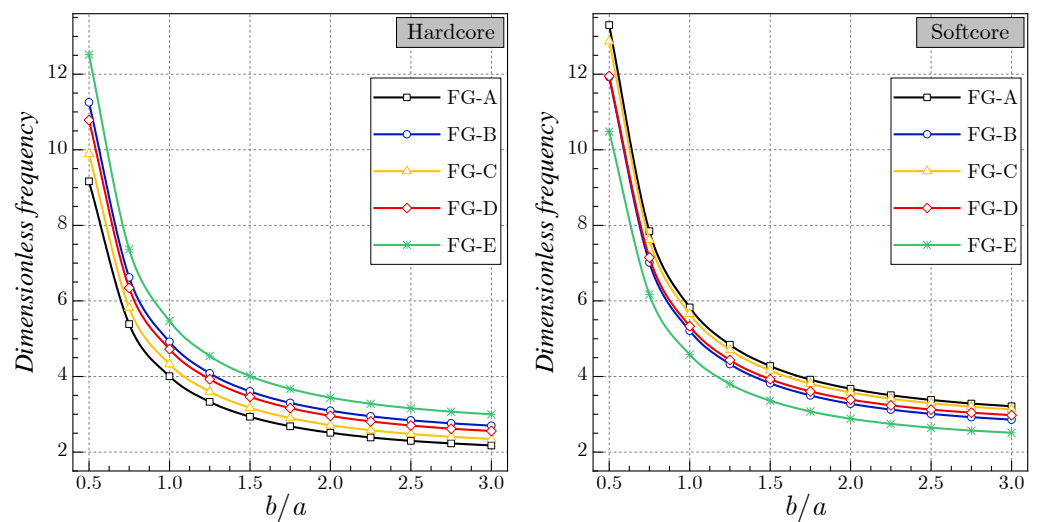


Figure 5. Effect of the exponents  $p$ ,  $k$  and  $e$  on the dimensionless frequencies of various types of coated shell (SSSS,  $b = a = 10h$ ,  $R_x/a = 5$ ,  $R_y/b = 5$ ).



**Figure 6.** Effect of the exponents  $p$  and  $k$  on the dimensionless frequencies of FG-C coated shell ( $SSSS, b = a = 10h, R_x/a = 5, R_y/b = 5$ ).



**Figure 7.** Effect of the aspect ratio on the dimensionless frequencies of various types of coated shell ( $SSSS, p = k = e = 2, a = 10h, R_x/a = 5, R_y/b = 5$ ).

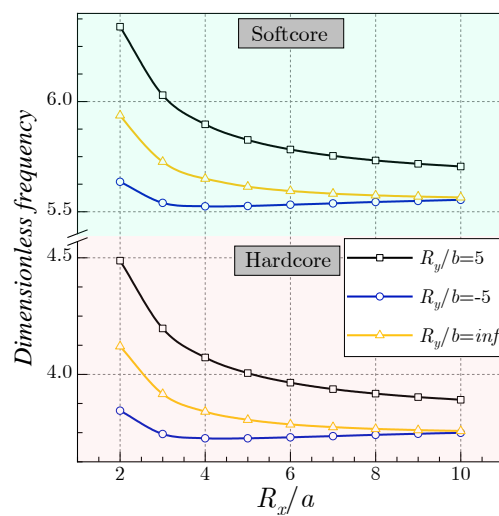


**Figure 8.** Effect of the radius of curvature on the dimensionless frequencies of FG-A coated shell ( $SSSS, p = k = e = 2, b = a = 10h$ ).

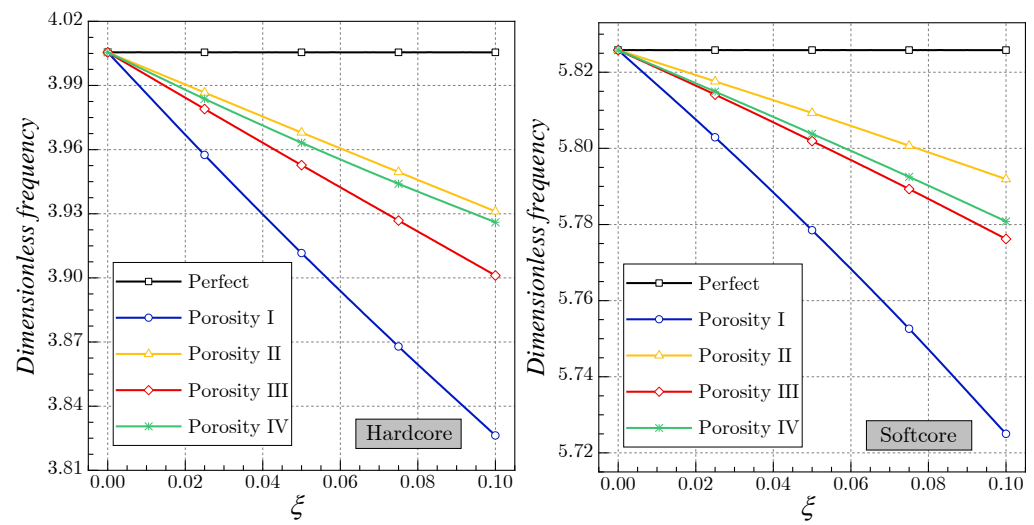


**Figure 9.** Effect of porosity coefficient on the dimensionless frequencies of FG-A coated shell ( $SSSS, p = k = e = 2, b = a = 10h, R_x/a = 5, R_y/b = 5$ ).

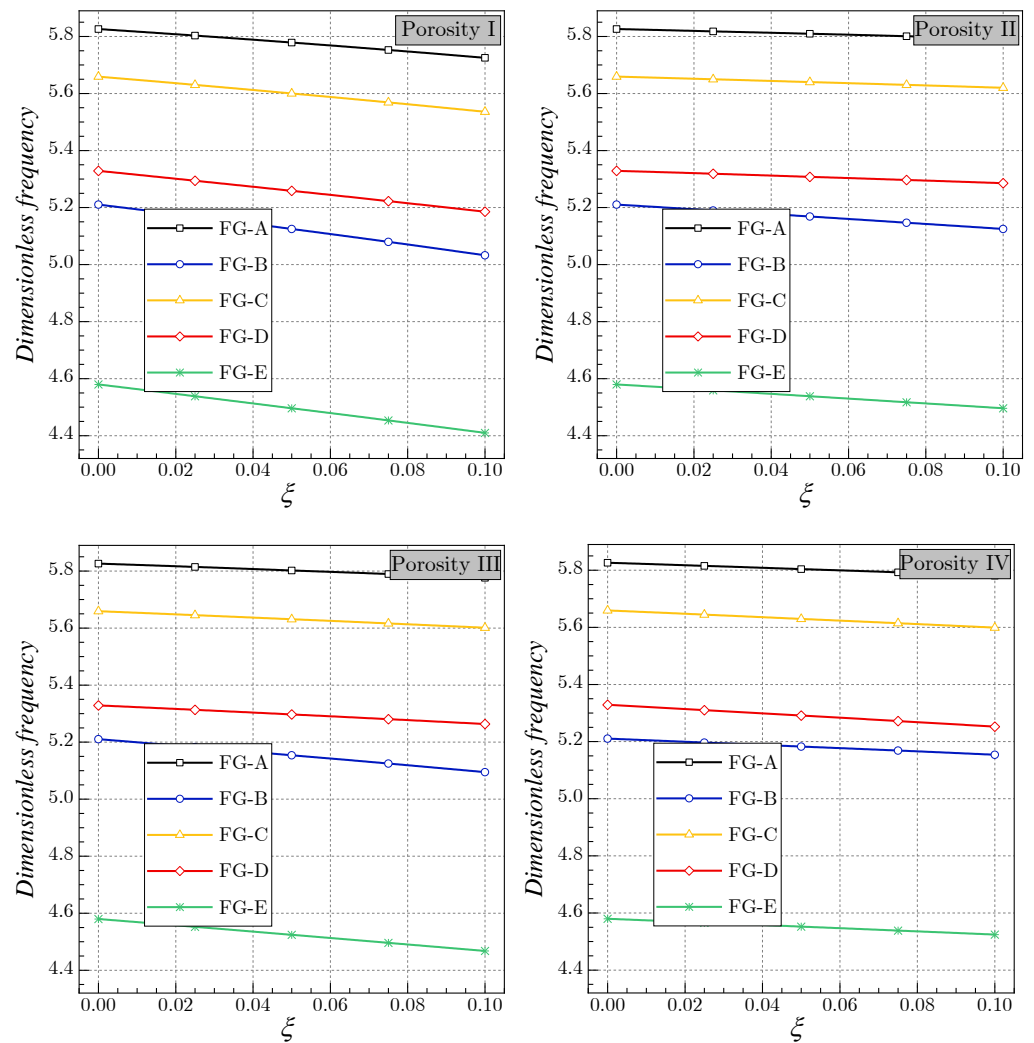


**Figure 10.** Effect of porosity coefficient on the dimensionless frequencies of various types of coated shell with softcore ( $SSSS, p = k = e = 2, b = a = 10h, R_x/a = 5, R_y/b = 5$ ).

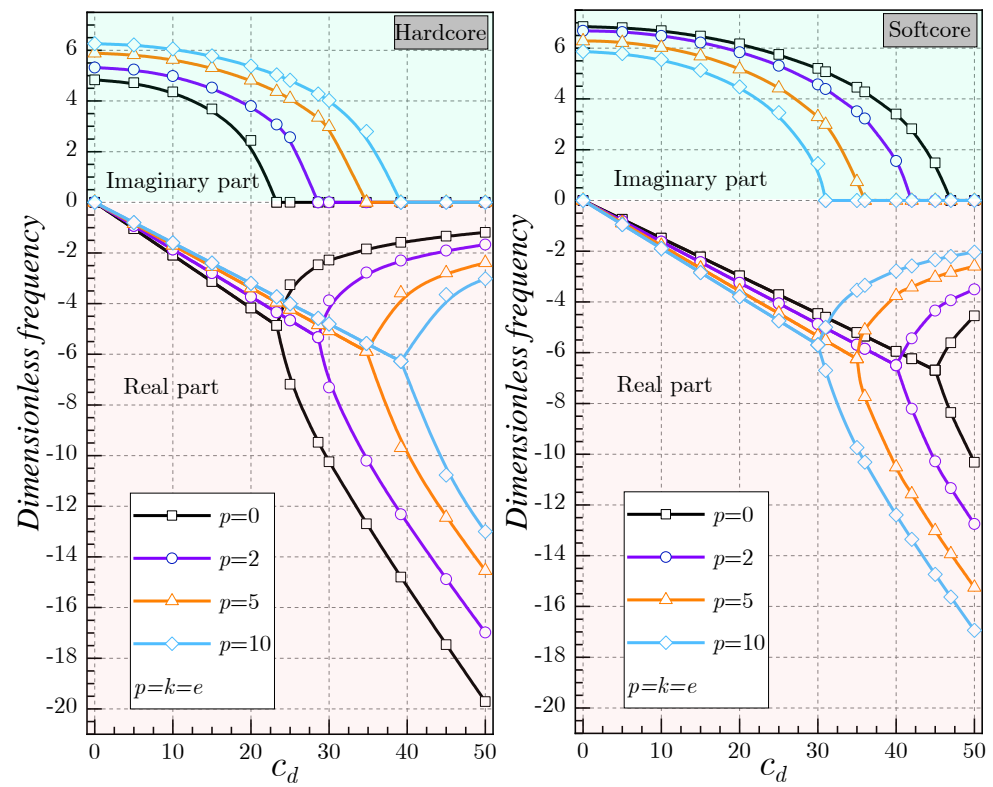


**Figure 11.** Effect of the damping coefficient on the dimensionless frequencies of FG-A coated shell ( $SSSS, b = a = 10h, R_x/a = 5, R_y/b = 5, K_w = K_s = 10$ ).

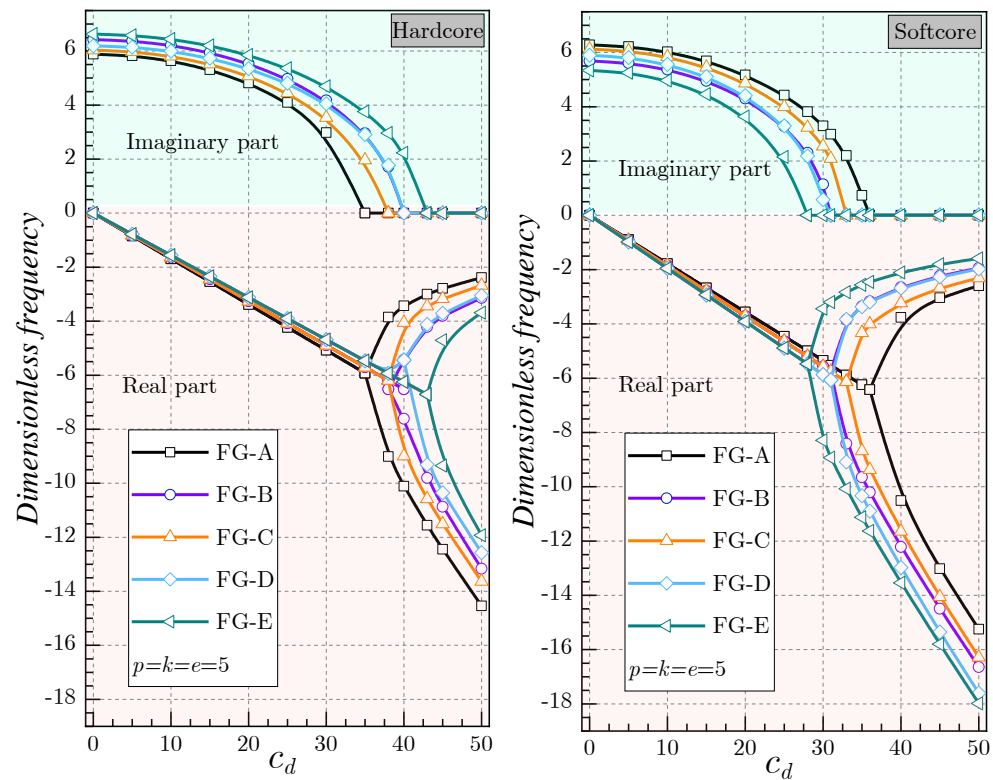


**Figure 12.** Effect of the damping coefficient on the dimensionless frequencies of various types of coated shell ( $SSSS, b = a = 10h, R_x/a = 5, R_y/b = 5, K_w = K_s = 10$ ).

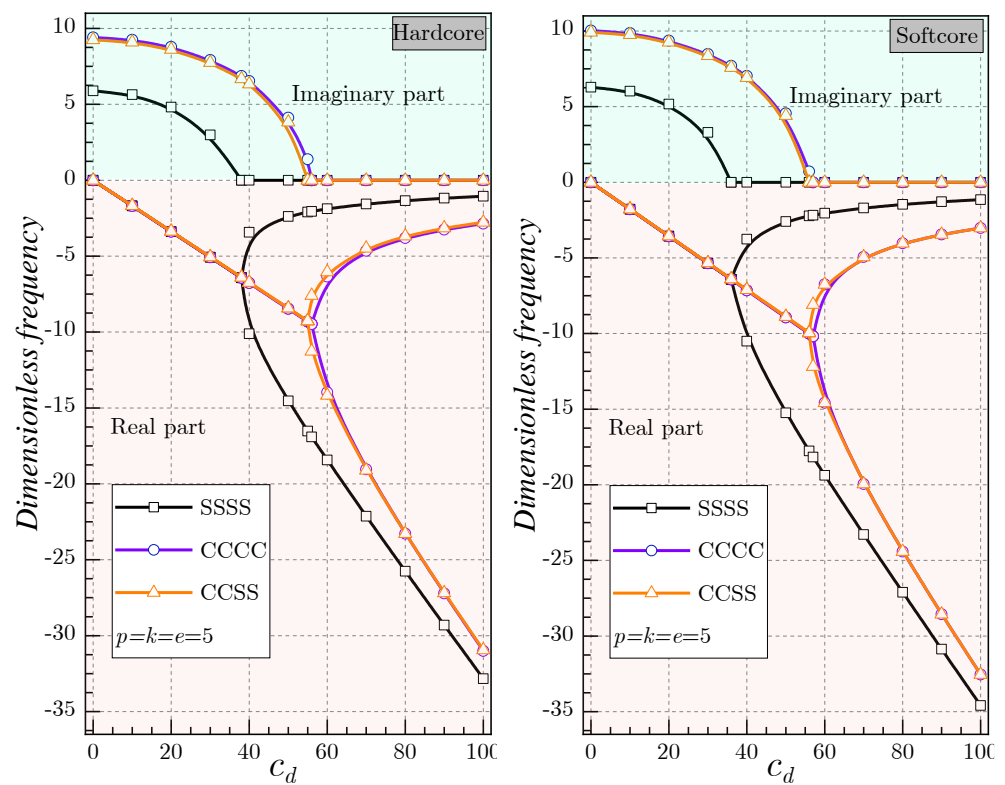


**Figure 13.** Effect of the damping coefficient on the dimensionless frequencies of FG-A coated shell subjected to different boundary conditions ( $b = a = 10h$ ,  $R_x/a = 5$ ,  $R_y/b = 5$ ,  $K_w = K_s = 10$ ).

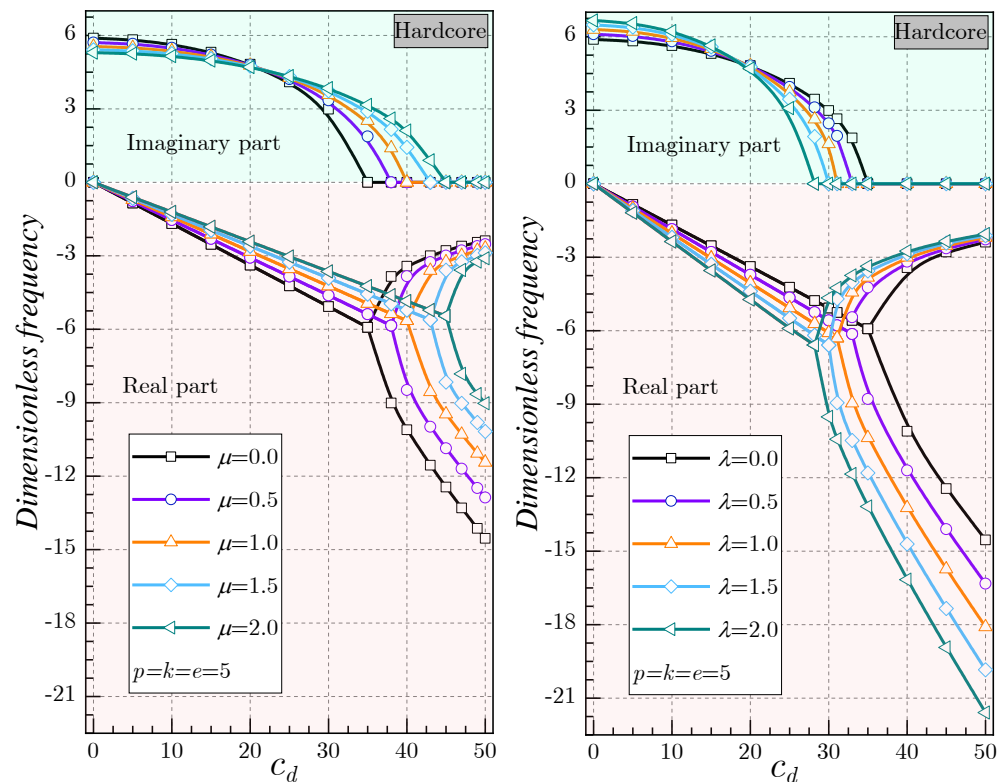


**Figure 14.** Effect of the damping coefficient on the dimensionless frequencies of FG-A coated nanoshell for different length-scale and nonlocal parameters ( $SSSS, b = a = 10h$ ,  $R_x/a = 5$ ,  $R_y/b = 5$ ,  $K_w = K_s = 10$ ).

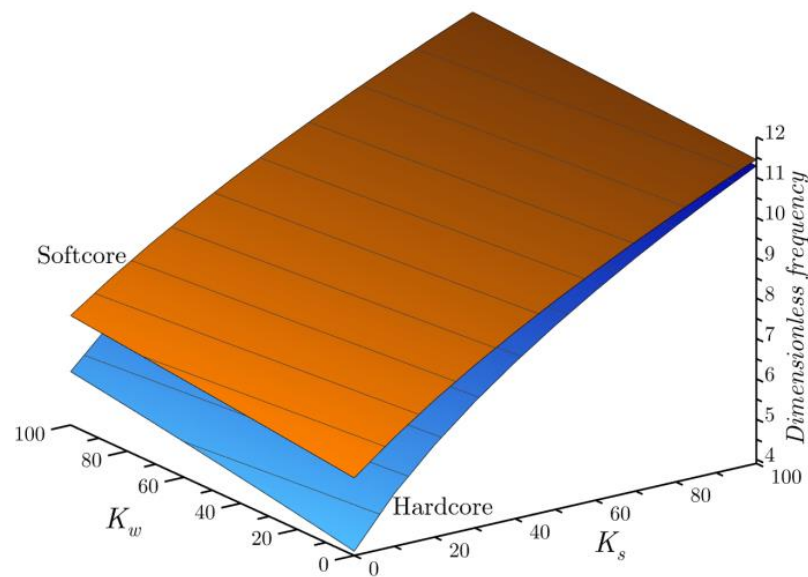


**Figure 15.** Effect of the elastic foundation parameters on the dimensionless frequencies of FG-A coated shell ( $SSSS, p = k = e = 2, b = a = 10h, R_x/a = 5, R_y/b = 5, C_d = 0$ ).

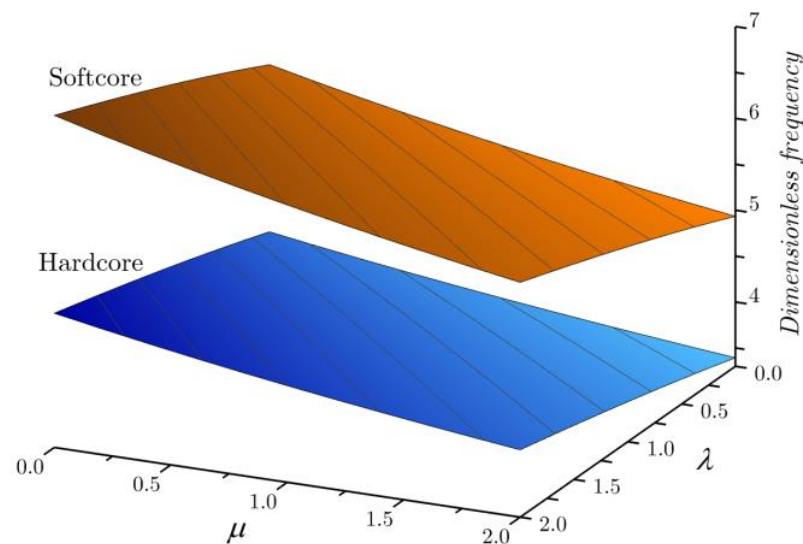


**Figure 16.** Effect of nonlocal and length-scale parameters on the dimensionless frequencies of FG-A coated shell ( $SSSS, p = k = e = 2, b = a = 10h, R_x/a = 5, R_y/b = 5$ ).

Figure 8 illustrates the effect of the radius of curvature  $R_x/a$  and  $R_y/b$  on the dimensionless frequencies of FG-A tri-coated shell for a constant inhomogeneity index  $p = k = e = 2$ . The augmentation of the radius of curvature  $R_x/a$  leads to a decrement in the dimensionless frequencies.

To demonstrate the action of porosities on the dimensionless frequencies of simply supported FG-A coated shells, Figure 9 is plotted. Four types of porosity distribution are examined by changing the value of the porosity coefficient  $\zeta$  from 0 (perfect shells) to 0.1. It is clear that the frequencies are influenced by the porosity coefficient  $\zeta$ , where the inclusion of porosities leads to a reduction in the shell stiffness; therefore, the frequencies decrease. By comparison of porosity distribution patterns, the “Porosity I” pattern has a significant impact, whereas the least impact is noted for the “Porosity II” pattern.

Figure 10 presents the action of various pattern distributions of porosity on the dimensionless frequencies of different schemes of a simply supported softcore coated spherical

shell. Regardless of the porosity pattern distributions, it is clear that the FG-E shells are more influenced by the coefficient of porosity than the other shell schemes.

The effect of the viscoelastic foundation on spherical hardcore/softcore FG coated shell is investigated in detail in Figures 11–14 by varying various material and geometric parameters. Figure 11 shows the effects of the damping coefficient of the viscoelastic medium and the material inhomogeneity parameters  $p$ ,  $k$  and  $e$  on the imaginary part of the eigenfrequency and the real part of the eigenfrequency of a simply supported coated FG spherical shell. The parameters of the Winkler/Pasternak foundation and the geometric parameters are taken as  $K_w = K_s = 10$  and  $b = a = 10h$ , respectively. As shown in this figure, the inclusion of the damping coefficient reduces the frequencies in a continuous manner, where the imaginary part of the eigenfrequency decreases as the damping coefficient increases. The higher values of inhomogeneity indexes of softcore FG coated shell (or lowest indexes of hardcore FG coated shell) lead to a smaller critical damping coefficient  $C_d$  in which the shell stiffness degrades, and the dimensionless frequencies decrease. The imaginary part of the eigenfrequency of the softcore shell becomes zero when the damping coefficient is  $C_d \cong 31, 36, 42$  and  $47$  for inhomogeneity indexes  $p = 10, 5, 2, 0$  ( $p = k = e$ ), respectively. For the hardcore FG shells, the imaginary part of the eigenfrequency becomes zero when  $C_d \cong 23.3, 25, 34.8$  and  $39.2$  for inhomogeneity indexes  $p = 0, 2, 5, 10$ , respectively.

The effect of the damping coefficient on the dimensionless frequencies of various types of coated shells is presented in Figure 12. It can be observed that, wherever the FG shell scheme is, the augmentation of the damping coefficient reduces the stiffness of the shell, and the imaginary eigenfrequencies degrade until a critical point in which the frequencies become zero.

Figure 13 shows the action of the damping coefficient on the dimensionless frequencies of an FG-A coated shell subjected to different boundary conditions. It is seen that the fully clamped (CCCC) FG coated shell has larger values of imaginary frequency than the CCSS and SSSS shells. Furthermore, there are three intersections in the real part of the eigenfrequency for the cases of  $C_d \cong 37$  for the SSSS shells,  $C_d \cong 55$  for the CCSS and CCCC shells. For example, in the first case of simply supported FG coated shells, the system is under-damped when  $C_d \leq 37$  and is over-damped when  $C_d \geq 37$ .

In Figure 14, the action of the damping coefficient on the dimensionless frequencies of a hardcore FG-A coated nanoshell for different length-scale and nonlocal parameters is plotted. It is seen that as the nonlocal parameter  $\mu$  increases, the value of the critical damping coefficient decreases. For more explanation, the rise in the nonlocal parameter decreases the interaction force between nanoshell atoms; therefore, the nanoshell becomes softer. On the other hand, the augmentation of the length-scale parameter  $\lambda$  leads to an increment in the shell stiffness; therefore, the critical damping coefficient increases.

The dimensionless frequencies of hardcore/softcore FG-A coated shells influenced by the Winkler/Pasternak elastic foundation are illustrated in Figure 15. The inclusion of the foundation improves the rigidity of the shells, where the increase in the parameters  $K_w$  and  $K_s$  lead to an augmentation in the values of the dimensionless frequency. In addition, the hardcore FG shell is more influenced by the foundation parameters than the softcore FG shell.

Figure 16 shows the effect of both the nonlocal parameter ( $\mu$ ) and the length-scale parameter ( $\lambda$ ) on the dimensionless frequencies of FG-A coated FG shells. It is observed that for both the softcore and hardcore coated FG shells, the dimensionless frequencies become larger as the nonlocal parameter ( $\mu$ ) decrease. This in turn means that the nonlocal effect has a stiffness-softening effect for both the softcore and hardcore coated FG shells. However, the dimensionless frequencies become smaller as the length-scale parameter ( $\lambda$ ) decreases. Clearly, the nonlocal effect has a stiffness-hardening effect for both the softcore and hard-core coated FG shells.

### 6. Conclusions

This paper focused on a new tri-coated functionally graded material (FGM) shell rested on a viscoelastic Winkler/Pasternak foundation. The analysis examined the free vibration response, taking into account the effects of porosities and microstructure. Two types of tri-coated FG shells, hardcore and softcore, were studied, and five distribution patterns were proposed. Additionally, four porosity distributions were analyzed. The research developed an analytical solution based on the Galerkin approach to cover different boundary conditions. Furthermore, a parametric analysis was carried out to explore the impact of various factors on the fundamental frequencies, including the types and distribution patterns of coated FG nanoshells, gradient material distribution, porosities, length-scale parameter (nonlocal), material scale parameter (gradient), nanoshell geometry, and elastic foundation variation. Finally, the study offers valuable insights into the design of FGM shells and their performance under different conditions:

- When the inhomogeneity indexes  $p, k$  and  $e$  increase, the hardcore FG shell becomes stiffer, while the softcore FG shell becomes less rigid.
- For any FG structure scheme, increasing the aspect ratio  $b/a$  and radius of curvature  $R/a$  results in a decrease in dimensionless frequencies.
- Including porosities into the FG shell decreases its stiffness, causing a reduction in the frequencies.
- The inclusion of the damping coefficient reduces the frequencies in a continuous manner, where the imaginary part of the eigenfrequency decreases as the damping coefficient increases.
- The inclusion of the Winkler/Pasternak foundations improves the rigidity of the shells, where the increase in various foundation parameters leads to an augmentation in the dimensionless frequency.

**Author Contributions:** E.E.G., project administration, funding acquisition, data curation. A.A.D., software, validation, formal analysis, investigation. S.K., formal analysis, investigation. A.M.A., software, visualization, data curation. E.M.B., conceptualization, formal analysis. M.A.E., conceptualization, methodology, review and editing. All authors have read and agreed to the published version of the manuscript.

**Funding:** This research was funded by the Institutional Fund Projects under Grant no. (IFPIP 1763-135-1443). Therefore, the authors gratefully acknowledge technical and financial support from the Ministry of Education and King Abdulaziz University, DSR, Jeddah, Saudi Arabia.

**Institutional Review Board Statement:** Not applicable.

**Informed Consent Statement:** Not applicable.

**Data Availability Statement:** Not applicable.

**Conflicts of Interest:** The authors declare no conflict of interest.

### Appendix A

Elementary stiffness matrix  $K_{ij}$ :

$$K_{11} = A_{11} \int_0^a \int_0^b \frac{\partial^3 X_m}{\partial x^3} Y_n \frac{\partial X_m}{\partial x} Y_n dx dy + A_{66} \int_0^a \int_0^b \frac{\partial X_m}{\partial x} \frac{\partial^2 Y_n}{\partial y^2} \frac{\partial X_m}{\partial x} Y_n dx dy - \lambda \left[ (A_{11} + A_{66}) \int_0^a \int_0^b \frac{\partial^3 X_m}{\partial x^3} \frac{\partial^2 Y_n}{\partial y^2} \frac{\partial X_m}{\partial x} Y_n dx dy + A_{11} \int_0^a \int_0^b \frac{\partial^5 X_m}{\partial x^5} Y_n \frac{\partial X_m}{\partial x} Y_n dx dy + A_{66} \int_0^a \int_0^b \frac{\partial X_m}{\partial x} \frac{\partial^4 Y_n}{\partial y^4} \frac{\partial X_m}{\partial x} Y_n dx dy \right]$$

$$K_{12} = (A_{12} + A_{66}) \left( \int_0^a \int_0^b \frac{\partial X_m}{\partial x} \frac{\partial^2 Y_n}{\partial y^2} \frac{\partial X_m}{\partial x} Y_n dx dy - \lambda \left[ \int_0^a \int_0^b \frac{\partial^3 X_m}{\partial x^3} \frac{\partial^2 Y_n}{\partial y^2} \frac{\partial X_m}{\partial x} Y_n dx dy + \int_0^a \int_0^b \frac{\partial X_m}{\partial x} \frac{\partial^4 Y_n}{\partial y^4} \frac{\partial X_m}{\partial x} Y_n dx dy \right] \right)$$

$$K_{13} = \left( \frac{A_{11}}{R_x} + \frac{A_{12}}{R_y} \right) \left( \int_0^a \int_0^b \frac{\partial X_m}{\partial x} Y_n \frac{\partial X_m}{\partial x} Y_n dx dy - \left[ \int_0^a \int_0^b \frac{\partial^3 X_m}{\partial x^3} Y_n \frac{\partial X_m}{\partial x} Y_n dx dy + \int_0^a \int_0^b \frac{\partial X_m}{\partial x} \frac{\partial^2 Y_n}{\partial y^2} \frac{\partial X_m}{\partial x} Y_n dx dy \right] \right) - B_{11} \int_0^a \int_0^b \frac{\partial^3 X_m}{\partial x^3} Y_n \frac{\partial X_m}{\partial x} Y_n dx dy - (B_{12} + 2B_{66}) \int_0^a \int_0^b \frac{\partial X_m}{\partial x} \frac{\partial^2 Y_n}{\partial y^2} \frac{\partial X_m}{\partial x} Y_n dx dy - \lambda \left[ -(B_{12} + 2B_{66} + B_{11}) \int_0^a \int_0^b \frac{\partial^3 X_m}{\partial x^3} \frac{\partial^2 Y_n}{\partial y^2} \frac{\partial X_m}{\partial x} Y_n dx dy - B_{11} \int_0^a \int_0^b \frac{\partial^5 X_m}{\partial x^5} Y_n \frac{\partial X_m}{\partial x} Y_n dx dy \right]$$

$$K_{14} = -C_{11} \int_0^a \int_0^b \frac{\partial^3 X_m}{\partial x^3} Y_n \frac{\partial X_m}{\partial x} Y_n dx dy - (C_{12} + 2C_{66}) \int_0^a \int_0^b \frac{\partial X_m}{\partial x} \frac{\partial^2 Y_n}{\partial y^2} \frac{\partial X_m}{\partial x} Y_n dx dy - \lambda \left[ -(B_{12} + 2B_{66} + B_{11}) \int_0^a \int_0^b \frac{\partial^3 X_m}{\partial x^3} \frac{\partial^2 Y_n}{\partial y^2} \frac{\partial X_m}{\partial x} Y_n dx dy - B_{11} \int_0^a \int_0^b \frac{\partial^5 X_m}{\partial x^5} Y_n \frac{\partial X_m}{\partial x} Y_n dx dy \right]$$

$$K_{21} = (A_{12} + A_{66}) \left( \int_0^a \int_0^b \frac{\partial^2 X_m}{\partial x^2} \frac{\partial Y_n}{\partial y} X_m \frac{\partial Y_n}{\partial y} dx dy - \lambda \left[ \int_0^a \int_0^b \frac{\partial^4 X_m}{\partial x^4} \frac{\partial Y_n}{\partial y} X_m \frac{\partial Y_n}{\partial y} dx dy + \int_0^a \int_0^b \frac{\partial^2 X_m}{\partial x^2} \frac{\partial^3 Y_n}{\partial y^3} X_m \frac{\partial Y_n}{\partial y} dx dy \right] \right)$$

$$K_{22} = A_{22} \int_0^a \int_0^b X_m \frac{\partial^3 Y_n}{\partial y^3} X_m \frac{\partial Y_n}{\partial y} dx dy + A_{66} \int_0^a \int_0^b \frac{\partial^2 X_m}{\partial x^2} \frac{\partial Y_n}{\partial y} X_m \frac{\partial Y_n}{\partial y} dx dy - \lambda \left[ (A_{22} + A_{66}) \int_0^a \int_0^b \frac{\partial^2 X_m}{\partial x^2} \frac{\partial^3 Y_n}{\partial y^3} X_m \frac{\partial Y_n}{\partial y} dx dy + A_{22} \int_0^a \int_0^b X_m \frac{\partial^5 Y_n}{\partial y^5} X_m \frac{\partial Y_n}{\partial y} dx dy + A_{66} \int_0^a \int_0^b \frac{\partial^4 X_m}{\partial x^4} \frac{\partial Y_n}{\partial y} X_m \frac{\partial Y_n}{\partial y} dx dy \right]$$

$$K_{23} = \left( \frac{A_{12}}{R_x} + \frac{A_{22}}{R_y} \right) \left( \int_0^a \int_0^b X_m \frac{\partial Y_n}{\partial y} X_m \frac{\partial Y_n}{\partial y} dx dy - \lambda \left[ \int_0^a \int_0^b \frac{\partial^2 X_m}{\partial x^2} \frac{\partial Y_n}{\partial y} X_m \frac{\partial Y_n}{\partial y} dx dy + \int_0^a \int_0^b X_m \frac{\partial^3 Y_n}{\partial y^3} X_m \frac{\partial Y_n}{\partial y} dx dy \right] \right) - B_{22} \int_0^a \int_0^b X_m \frac{\partial^3 Y_n}{\partial y^3} X_m \frac{\partial Y_n}{\partial y} dx dy - (B_{12} + 2B_{66}) \int_0^a \int_0^b \frac{\partial X_m}{\partial x} \frac{\partial^2 Y_n}{\partial y^2} X_m \frac{\partial Y_n}{\partial y} dx dy - \lambda \left[ -B_{22} \left( \int_0^a \int_0^b \frac{\partial^2 X_m}{\partial x^2} \frac{\partial^3 Y_n}{\partial y^3} X_m \frac{\partial Y_n}{\partial y} dx dy + \int_0^a \int_0^b X_m \frac{\partial^5 Y_n}{\partial y^5} X_m \frac{\partial Y_n}{\partial y} dx dy \right) - (B_{12} + 2B_{66}) \left( \int_0^a \int_0^b \frac{\partial^3 X_m}{\partial x^3} \frac{\partial^2 Y_n}{\partial y^2} X_m \frac{\partial Y_n}{\partial y} dx dy + \int_0^a \int_0^b \frac{\partial X_m}{\partial x} \frac{\partial^4 Y_n}{\partial y^4} X_m \frac{\partial Y_n}{\partial y} dx dy \right) \right]$$

$$K_{24} = -C_{22} \int_0^a \int_0^b X_m \frac{\partial^3 Y_n}{\partial y^3} X_m \frac{\partial Y_n}{\partial y} dx dy - (C_{12} + 2C_{66}) \int_0^a \int_0^b \frac{\partial^2 X_m}{\partial x^2} \frac{\partial Y_n}{\partial y} X_m \frac{\partial Y_n}{\partial y} dx dy - \lambda \left[ -C_{22} \left( \int_0^a \int_0^b \frac{\partial^2 X_m}{\partial x^2} \frac{\partial^3 Y_n}{\partial y^3} X_m \frac{\partial Y_n}{\partial y} dx dy + \int_0^a \int_0^b X_m \frac{\partial^5 Y_n}{\partial y^5} X_m \frac{\partial Y_n}{\partial y} dx dy \right) - (C_{12} + 2C_{66}) \left( \int_0^a \int_0^b \frac{\partial^4 X_m}{\partial x^4} \frac{\partial Y_n}{\partial y} X_m \frac{\partial Y_n}{\partial y} dx dy + \int_0^a \int_0^b \frac{\partial^2 X_m}{\partial x^2} \frac{\partial^3 Y_n}{\partial y^3} X_m \frac{\partial Y_n}{\partial y} dx dy \right) \right]$$

$$\begin{aligned}
 K_{31} = & -\left(\frac{A_{11}}{R_x} + \frac{A_{12}}{R_y}\right) \left( \int_0^a \int_0^b \frac{\partial^2 X_n}{\partial x^2} Y_n X_m Y_n dx dy - \lambda \left[ \int_0^a \int_0^b \frac{\partial^4 X_n}{\partial x^4} Y_n X_m Y_n dx dy + \int_0^a \int_0^b \frac{\partial^2 X_n}{\partial x^2} \frac{\partial^2 Y_n}{\partial y^2} X_m Y_n dx dy \right] \right) \\
 & + B_{11} \int_0^a \int_0^b \frac{\partial^4 X_n}{\partial x^4} Y_n X_m Y_n dx dy + (B_{12} + 2B_{66}) \int_0^a \int_0^b \frac{\partial^2 X_m}{\partial x^2} \frac{\partial^2 Y_n}{\partial y^2} X_m Y_n dx dy \\
 & - \lambda \left[ B_{11} \int_0^a \int_0^b \frac{\partial^6 X_n}{\partial x^6} Y_n X_m Y_n dx dy + (B_{11} + B_{12} + 2B_{66}) \int_0^a \int_0^b \frac{\partial^4 X_m}{\partial x^4} \frac{\partial^2 Y_n}{\partial y^2} X_m Y_n dx dy \right. \\
 & \left. + (B_{12} + 2B_{66}) \int_0^a \int_0^b \frac{\partial^2 X_m}{\partial x^2} \frac{\partial^4 Y_n}{\partial y^4} X_m Y_n dx dy \right]
 \end{aligned}$$

$$\begin{aligned}
 K_{32} = & -\left(\frac{A_{12}}{R_x} + \frac{A_{22}}{R_y}\right) \left( \int_0^a \int_0^b X_m \frac{\partial^2 Y_n}{\partial y^2} X_m Y_n dx dy \right. \\
 & \left. - \lambda \left[ \int_0^a \int_0^b \frac{\partial^2 X_m}{\partial x^2} \frac{\partial^2 Y_n}{\partial y^2} X_m Y_n dx dy + \int_0^a \int_0^b X_m \frac{\partial^4 Y_n}{\partial y^4} X_m Y_n dx dy \right] \right) \\
 & + B_{22} \int_0^a \int_0^b X_m \frac{\partial^4 Y_n}{\partial y^4} X_m Y_n dx dy + (B_{12} + 2B_{66}) \int_0^a \int_0^b \frac{\partial^2 X_m}{\partial x^2} \frac{\partial^2 Y_n}{\partial y^2} X_m Y_n dx dy \\
 & - \lambda \left[ (B_{22} + B_{12} + 2B_{66}) \int_0^a \int_0^b \frac{\partial^2 X_m}{\partial x^2} \frac{\partial^4 Y_n}{\partial y^4} X_m Y_n dx dy \right. \\
 & \left. + (B_{12} + 2B_{66}) \int_0^a \int_0^b \frac{\partial^4 X_m}{\partial x^4} \frac{\partial^2 Y_n}{\partial y^2} X_m Y_n dx dy + B_{22} \int_0^a \int_0^b X_m \frac{\partial^6 Y_n}{\partial y^6} X_m Y_n dx dy \right]
 \end{aligned}$$

$$\begin{aligned}
 K_{33} = & 2\left(\frac{B_{11}}{R_x} + \frac{B_{12}}{R_y}\right) \left( \int_0^a \int_0^b \frac{\partial^2 X_n}{\partial x^2} Y_n X_m Y_n dx dy - \lambda \left[ \int_0^a \int_0^b \frac{\partial^4 X_m}{\partial x^4} Y_n X_m Y_n dx dy + \int_0^a \int_0^b \frac{\partial^2 X_n}{\partial x^2} \frac{\partial^2 Y_n}{\partial y^2} X_m Y_n dx dy \right] \right) \\
 & + 2\left(\frac{B_{12}}{R_x} + \frac{B_{22}}{R_y}\right) \left( \int_0^a \int_0^b X_m \frac{\partial^2 Y_n}{\partial y^2} X_m Y_n dx dy - \lambda \left[ \int_0^a \int_0^b \frac{\partial^2 X_m}{\partial x^2} \frac{\partial^2 Y_n}{\partial y^2} X_m Y_n dx dy + \int_0^a \int_0^b X_m \frac{\partial^4 Y_n}{\partial y^4} X_m Y_n dx dy \right] \right) \\
 & - \left(\frac{A_{11}}{R_x^2} + 2\frac{A_{12}}{R_x R_y} + \frac{A_{22}}{R_y^2}\right) \left( \int_0^a \int_0^b X_m Y_n X_m Y_n dx dy - \lambda \left[ \int_0^a \int_0^b \frac{\partial^2 X_m}{\partial x^2} Y_n X_m Y_n dx dy + \int_0^a \int_0^b X_m \frac{\partial^2 Y_n}{\partial y^2} X_m Y_n dx dy \right] \right) \\
 & - D_{11} \int_0^a \int_0^b \frac{\partial^4 X_m}{\partial x^4} Y_n X_m Y_n dx dy - D_{22} \left( \int_0^a \int_0^b X_m \frac{\partial^4 Y_n}{\partial y^4} X_m Y_n dx dy \right) - 2(D_{12} + 2D_{66}) \int_0^a \int_0^b \frac{\partial^2 X_m}{\partial x^2} \frac{\partial^2 Y_n}{\partial y^2} X_m Y_n dx dy \\
 & - \lambda \left[ -D_{11} \int_0^a \int_0^b \frac{\partial^6 X_m}{\partial x^6} Y_n X_m Y_n dx dy - D_{22} \int_0^a \int_0^b X_m \frac{\partial^6 Y_n}{\partial y^6} X_m Y_n dx dy \right. \\
 & \left. - (D_{11} + 2D_{12} + 4D_{66}) \int_0^a \int_0^b \frac{\partial^4 X_m}{\partial x^4} \frac{\partial^2 Y_n}{\partial y^2} X_m Y_n dx dy - (D_{22} + 2D_{12} + 4D_{66}) \int_0^a \int_0^b \frac{\partial^2 X_m}{\partial x^2} \frac{\partial^4 Y_n}{\partial y^4} X_m Y_n dx dy \right]
 \end{aligned}$$

$$\begin{aligned}
 K_{34} = & -\left(\frac{C_{11}}{R_x} + \frac{C_{12}}{R_y}\right) \left( \int_0^a \int_0^b \frac{\partial^2 X_n}{\partial x^2} Y_n X_m Y_n dx dy - \lambda \left[ \int_0^a \int_0^b \frac{\partial^4 X_m}{\partial x^4} Y_n X_m Y_n dx dy + \int_0^a \int_0^b \frac{\partial^2 X_n}{\partial x^2} \frac{\partial^2 Y_n}{\partial y^2} X_m Y_n dx dy \right] \right) \\
 & - \left(\frac{C_{12}}{R_x} + \frac{C_{22}}{R_y}\right) \left( \int_0^a \int_0^b X_m \frac{\partial^2 Y_n}{\partial y^2} X_m Y_n dx dy \right. \\
 & \left. - \lambda \left[ \int_0^a \int_0^b \frac{\partial^2 X_m}{\partial x^2} \frac{\partial^2 Y_n}{\partial y^2} X_m Y_n dx dy + \int_0^a \int_0^b X_m \frac{\partial^4 Y_n}{\partial y^4} X_m Y_n dx dy \right] \right) - E_{11} \int_0^a \int_0^b \frac{\partial^4 X_m}{\partial x^4} Y_n X_m Y_n dx dy \\
 & - E_{22} \left( \int_0^a \int_0^b X_m \frac{\partial^4 Y_n}{\partial y^4} X_m Y_n dx dy \right) - 2(E_{12} + 2E_{66}) \int_0^a \int_0^b \frac{\partial^2 X_m}{\partial x^2} \frac{\partial^2 Y_n}{\partial y^2} X_m Y_n dx dy \\
 & - \lambda \left[ -E_{11} \int_0^a \int_0^b \frac{\partial^6 X_m}{\partial x^6} Y_n X_m Y_n dx dy - E_{22} \int_0^a \int_0^b X_m \frac{\partial^6 Y_n}{\partial y^6} X_m Y_n dx dy \right. \\
 & \left. - (E_{11} + 2E_{12} + 4E_{66}) \int_0^a \int_0^b \frac{\partial^4 X_m}{\partial x^4} \frac{\partial^2 Y_n}{\partial y^2} X_m Y_n dx dy \right. \\
 & \left. - (E_{22} + 2E_{12} + 4E_{66}) \int_0^a \int_0^b \frac{\partial^2 X_m}{\partial x^2} \frac{\partial^4 Y_n}{\partial y^4} X_m Y_n dx dy \right]
 \end{aligned}$$

$$\begin{aligned}
 K_{41} &= C_{11} \int_0^a \int_0^b \frac{\partial^4 X_m}{\partial x^4} Y_n X_m Y_n dx dy + (C_{12} + 2C_{66}) \int_0^a \int_0^b \frac{\partial^2 X_m}{\partial x^2} \frac{\partial^2 Y_n}{\partial y^2} X_m Y_n dx dy \\
 &\quad - \lambda \left[ C_{11} \int_0^a \int_0^b \frac{\partial^6 X_m}{\partial x^6} Y_n X_m Y_n dx dy + (C_{12} + 2C_{66}) \int_0^a \int_0^b \frac{\partial^2 X_m}{\partial x^2} \frac{\partial^4 Y_n}{\partial y^4} X_m Y_n dx dy \right. \\
 &\quad \left. + (C_{11} + C_{12} + 2C_{66}) \left( \int_0^a \int_0^b \frac{\partial^4 X_m}{\partial x^4} \frac{\partial^2 Y_n}{\partial y^2} X_m Y_n dx dy \right) \right] \\
 K_{42} &= C_{22} \int_0^a \int_0^b X_m \frac{\partial^4 Y_n}{\partial y^4} X_m Y_n dx dy + (C_{12} + 2C_{66}) \int_0^a \int_0^b \frac{\partial^2 X_m}{\partial x^2} \frac{\partial^2 Y_n}{\partial y^2} X_m Y_n dx dy \\
 &\quad - \lambda \left[ C_{22} \int_0^a \int_0^b X_m \frac{\partial^6 Y_n}{\partial y^6} X_m Y_n dx dy \right. \\
 &\quad \left. + (C_{12} + 2C_{66}) \int_0^a \int_0^b \frac{\partial^4 X_m}{\partial x^4} \frac{\partial^2 Y_n}{\partial y^2} X_m Y_n dx dy (C_{22} + C_{12} + 2C_{66}) \int_0^a \int_0^b \frac{\partial^2 X_m}{\partial x^2} \frac{\partial^4 Y_n}{\partial y^4} X_m Y_n dx dy \right] \\
 K_{43} &= - \left( \frac{C_{11}}{R_x} + \frac{C_{12}}{R_y} \right) \left( \int_0^a \int_0^b \frac{\partial X_m}{\partial x} Y_n \frac{\partial X_m}{\partial x} Y_n dx dy - \lambda \left[ \int_0^a \int_0^b \frac{\partial^3 X_m}{\partial x^3} Y_n \frac{\partial X_m}{\partial x} Y_n dx dy + \int_0^a \int_0^b \frac{\partial X_m}{\partial x} \frac{\partial^2 Y_n}{\partial y^2} \frac{\partial X_m}{\partial x} Y_n dx dy \right] \right) \\
 &\quad - \left( \frac{C_{12}}{R_x} + \frac{C_{22}}{R_y} \right) \left( \int_0^a \int_0^b X_m \frac{\partial Y_n}{\partial y} X_m \frac{\partial Y_n}{\partial y} dx dy \right. \\
 &\quad \left. - \lambda \left[ \int_0^a \int_0^b \frac{\partial^2 X_m}{\partial x^2} \frac{\partial Y_n}{\partial y} X_m \frac{\partial Y_n}{\partial y} dx dy + \int_0^a \int_0^b X_m \frac{\partial^3 Y_n}{\partial y^3} X_m \frac{\partial Y_n}{\partial y} dx dy \right] \right) - E_{11} \int_0^a \int_0^b \frac{\partial^4 X_m}{\partial x^4} Y_n X_m Y_n dx dy \\
 &\quad - E_{22} \left( \int_0^a \int_0^b X_m \frac{\partial^4 Y_n}{\partial y^4} X_m Y_n dx dy \right) - 2(E_{12} + 2E_{66}) \int_0^a \int_0^b \frac{\partial^2 X_m}{\partial x^2} \frac{\partial^2 Y_n}{\partial y^2} X_m Y_n dx dy \\
 &\quad - \lambda \left[ -E_{11} \int_0^a \int_0^b \frac{\partial^6 X_m}{\partial x^6} Y_n X_m Y_n dx dy - E_{22} \int_0^a \int_0^b X_m \frac{\partial^6 Y_n}{\partial y^6} X_m Y_n dx dy \right. \\
 &\quad \left. - (E_{11} + 2E_{12} + 4E_{66}) \int_0^a \int_0^b \frac{\partial^4 X_m}{\partial x^4} \frac{\partial^2 Y_n}{\partial y^2} X_m Y_n dx dy \right. \\
 &\quad \left. - (E_{22} + 2E_{12} + 4E_{66}) \int_0^a \int_0^b \frac{\partial^2 X_m}{\partial x^2} \frac{\partial^4 Y_n}{\partial y^4} X_m Y_n dx dy \right] \\
 K_{44} &= -F_{11} \int_0^a \int_0^b \frac{\partial^4 X_m}{\partial x^4} Y_n X_m Y_n dx dy - F_{22} \left( \int_0^a \int_0^b X_m \frac{\partial^4 Y_n}{\partial y^4} X_m Y_n dx dy \right) - 2(F_{12} + 2F_{66}) \int_0^a \int_0^b \frac{\partial^2 X_m}{\partial x^2} \frac{\partial^2 Y_n}{\partial y^2} X_m Y_n dx dy \\
 &\quad + J_{44} \int_0^a \int_0^b X_m \frac{\partial^2 Y_n}{\partial y^2} X_m Y_n dx dy + J_{55} \int_0^a \int_0^b \frac{\partial^2 X_m}{\partial x^2} Y_n X_m Y_n dx dy \\
 &\quad - \lambda \left[ -F_{11} \int_0^a \int_0^b \frac{\partial^6 X_m}{\partial x^6} Y_n X_m Y_n dx dy - F_{22} \int_0^a \int_0^b X_m \frac{\partial^6 Y_n}{\partial y^6} X_m Y_n dx dy \right. \\
 &\quad \left. - (F_{11} + 2F_{12} + 4F_{66}) \int_0^a \int_0^b \frac{\partial^4 X_m}{\partial x^4} \frac{\partial^2 Y_n}{\partial y^2} X_m Y_n dx dy - (F_{22} + 2F_{12} + 4F_{66}) \int_0^a \int_0^b \frac{\partial^2 X_m}{\partial x^2} \frac{\partial^4 Y_n}{\partial y^4} X_m Y_n dx dy \right. \\
 &\quad \left. + J_{44} \int_0^a \int_0^b X_m \frac{\partial^4 Y_n}{\partial y^4} X_m Y_n dx dy + J_{55} \int_0^a \int_0^b \frac{\partial^4 X_m}{\partial x^4} Y_n X_m Y_n dx dy \right. \\
 &\quad \left. + (J_{44} + J_{55}) \int_0^a \int_0^b \frac{\partial^2 X_m}{\partial x^2} \frac{\partial^2 Y_n}{\partial y^2} X_m Y_n dx dy \right]
 \end{aligned}$$

Elementary mass matrix  $M_{ij}$ :

$$\begin{aligned}
 M_{11} &= \left( I_0 + 2 \frac{I_1}{R_x} + \frac{I_3}{R_y^2} \right) \left[ \int_0^a \int_0^b \frac{\partial X_m}{\partial x} Y_n \frac{\partial X_m}{\partial x} Y_n dx dy - \mu \left( \int_0^a \int_0^b \frac{\partial^3 X_m}{\partial x^3} Y_n \frac{\partial X_m}{\partial x} Y_n dx dy + \int_0^a \int_0^b \frac{\partial X_m}{\partial x} \frac{\partial^2 Y_n}{\partial y^2} \frac{\partial X_m}{\partial x} Y_n dx dy \right) \right] \\
 M_{13} &= - \left( I_1 + \frac{I_2}{R_x} \right) \left[ \int_0^a \int_0^b \frac{\partial X_m}{\partial x} Y_n \frac{\partial X_m}{\partial x} Y_n dx dy - \mu \left( \int_0^a \int_0^b \frac{\partial^3 X_m}{\partial x^3} Y_n \frac{\partial X_m}{\partial x} Y_n dx dy + \int_0^a \int_0^b \frac{\partial X_m}{\partial x} \frac{\partial^2 Y_n}{\partial y^2} \frac{\partial X_m}{\partial x} Y_n dx dy \right) \right] \\
 M_{14} &= \left( I_3 + \frac{I_4}{R_x} \right) \left[ \int_0^a \int_0^b \frac{\partial X_m}{\partial x} Y_n \frac{\partial X_m}{\partial x} Y_n dx dy - \mu \left( \int_0^a \int_0^b \frac{\partial^3 X_m}{\partial x^3} Y_n \frac{\partial X_m}{\partial x} Y_n dx dy + \int_0^a \int_0^b \frac{\partial X_m}{\partial x} \frac{\partial^2 Y_n}{\partial y^2} \frac{\partial X_m}{\partial x} Y_n dx dy \right) \right]
 \end{aligned}$$

$$\begin{aligned}
 M_{22} &= \left( I_0 + 2 \frac{I_1}{R_y} + \frac{I_2}{R_y^2} \right) \left[ \int_0^a \int_0^b X_m \frac{\partial Y_n}{\partial y} X_m \frac{\partial Y_n}{\partial y} dx dy - \mu \left( \int_0^a \int_0^b \frac{\partial^2 X_m}{\partial x^2} \frac{\partial Y_n}{\partial y} X_m \frac{\partial Y_n}{\partial y} dx dy + \int_0^a \int_0^b X_m \frac{\partial^3 Y_n}{\partial y^3} X_m \frac{\partial Y_n}{\partial y} dx dy \right) \right] \\
 M_{23} &= - \left( I_1 + \frac{I_2}{R_y} \right) \left[ \int_0^a \int_0^b X_m \frac{\partial Y_n}{\partial y} X_m \frac{\partial Y_n}{\partial y} dx dy - \mu \left( \int_0^a \int_0^b \frac{\partial^2 X_m}{\partial x^2} \frac{\partial Y_n}{\partial y} X_m \frac{\partial Y_n}{\partial y} dx dy + \int_0^a \int_0^b X_m \frac{\partial^3 Y_n}{\partial y^3} X_m \frac{\partial Y_n}{\partial y} dx dy \right) \right] \\
 M_{24} &= - \left( I_3 + \frac{I_4}{R_y} \right) \left[ \int_0^a \int_0^b X_m \frac{\partial Y_n}{\partial y} X_m \frac{\partial Y_n}{\partial y} dx dy - \mu \left( \int_0^a \int_0^b \frac{\partial^2 X_m}{\partial x^2} \frac{\partial Y_n}{\partial y} X_m \frac{\partial Y_n}{\partial y} dx dy + \int_0^a \int_0^b X_m \frac{\partial^3 Y_n}{\partial y^3} X_m \frac{\partial Y_n}{\partial y} dx dy \right) \right] \\
 M_{31} &= \left( I_1 + \frac{I_2}{R_x} \right) \left[ \int_0^a \int_0^b \frac{\partial^2 X_m}{\partial x^2} Y_n X_m Y_n dx dy - \mu \left( \int_0^a \int_0^b \frac{\partial^4 X_m}{\partial x^4} Y_n X_m Y_n dx dy + \int_0^a \int_0^b \frac{\partial^2 X_m}{\partial x^2} \frac{\partial^2 Y_n}{\partial y^2} X_m Y_n dx dy \right) \right] \\
 M_{32} &= \left( I_1 + \frac{I_2}{R_y} \right) I_1 \left[ \int_0^a \int_0^b X_m \frac{\partial^2 Y_n}{\partial y^2} X_m Y_n dx dy - \mu \left( \int_0^a \int_0^b \frac{\partial^2 X_m}{\partial x^2} \frac{\partial^2 Y_n}{\partial y^2} X_m Y_n dx dy + \int_0^a \int_0^b X_m \frac{\partial^4 Y_n}{\partial y^4} X_m Y_n dx dy \right) \right] \\
 M_{33} &= I_0 \left[ \int_0^a \int_0^b X_m Y_n X_m Y_n dx dy - \mu \left( \int_0^a \int_0^b \frac{\partial^2 X_m}{\partial x^2} Y_n X_m Y_n dx dy + \int_0^a \int_0^b X_m \frac{\partial^2 Y_n}{\partial y^2} X_m Y_n dx dy \right) \right] \\
 &\quad - I_2 \left[ \int_0^a \int_0^b \frac{\partial^2 X_m}{\partial x^2} Y_n X_m Y_n dx dy + \int_0^a \int_0^b X_m \frac{\partial^2 Y_n}{\partial y^2} X_m Y_n dx dy \right] \\
 &\quad - \mu \left( \int_0^a \int_0^b \frac{\partial^4 X_m}{\partial x^4} Y_n X_m Y_n dx dy + 2 \int_0^a \int_0^b \frac{\partial^2 X_m}{\partial x^2} \frac{\partial^2 Y_n}{\partial y^2} X_m Y_n dx dy + \int_0^a \int_0^b X_m \frac{\partial^4 Y_n}{\partial y^4} X_m Y_n dx dy \right) \Big] \\
 M_{34} &= -I_4 \left[ \int_0^a \int_0^b \frac{\partial^2 X_m}{\partial x^2} Y_n X_m Y_n dx dy + \int_0^a \int_0^b X_m \frac{\partial^2 Y_n}{\partial y^2} X_m Y_n dx dy \right. \\
 &\quad \left. - \mu \left( \int_0^a \int_0^b \frac{\partial^4 X_m}{\partial x^4} Y_n X_m Y_n dx dy + 2 \int_0^a \int_0^b \frac{\partial^2 X_m}{\partial x^2} \frac{\partial^2 Y_n}{\partial y^2} X_m Y_n dx dy + \int_0^a \int_0^b X_m \frac{\partial^4 Y_n}{\partial y^4} X_m Y_n dx dy \right) \right] \\
 M_{41} &= \left( I_3 + \frac{I_4}{R_x} \right) \left[ \int_0^a \int_0^b \frac{\partial^2 X_m}{\partial x^2} Y_n X_m Y_n dx dy - \mu \left( \int_0^a \int_0^b \frac{\partial^4 X_m}{\partial x^4} Y_n X_m Y_n dx dy + \int_0^a \int_0^b \frac{\partial^2 X_m}{\partial x^2} \frac{\partial^2 Y_n}{\partial y^2} X_m Y_n dx dy \right) \right] \\
 M_{42} &= \left( I_3 + \frac{I_4}{R_y} \right) \left[ \int_0^a \int_0^b \frac{\partial^2 X_m}{\partial x^2} Y_n X_m Y_n dx dy - \mu \left( \int_0^a \int_0^b \frac{\partial^2 X_m}{\partial x^2} \frac{\partial^2 Y_n}{\partial y^2} X_m Y_n dx dy + \int_0^a \int_0^b X_m \frac{\partial^4 Y_n}{\partial y^4} X_m Y_n dx dy \right) \right] \\
 M_{43} &= -I_4 \left[ \int_0^a \int_0^b \frac{\partial^2 X_m}{\partial x^2} Y_n X_m Y_n dx dy + \int_0^a \int_0^b X_m \frac{\partial^2 Y_n}{\partial y^2} X_m Y_n dx dy \right. \\
 &\quad \left. - \mu \left( \int_0^a \int_0^b \frac{\partial^4 X_m}{\partial x^4} Y_n X_m Y_n dx dy + 2 \int_0^a \int_0^b \frac{\partial^2 X_m}{\partial x^2} \frac{\partial^2 Y_n}{\partial y^2} X_m Y_n dx dy + \int_0^a \int_0^b X_m \frac{\partial^4 Y_n}{\partial y^4} X_m Y_n dx dy \right) \right] \\
 M_{44} &= -I_5 \left[ \int_0^a \int_0^b \frac{\partial^2 X_m}{\partial x^2} Y_n X_m Y_n dx dy + \int_0^a \int_0^b X_m \frac{\partial^2 Y_n}{\partial y^2} X_m Y_n dx dy \right. \\
 &\quad \left. - \mu \left( \int_0^a \int_0^b \frac{\partial^4 X_m}{\partial x^4} Y_n X_m Y_n dx dy + 2 \int_0^a \int_0^b \frac{\partial^2 X_m}{\partial x^2} \frac{\partial^2 Y_n}{\partial y^2} X_m Y_n dx dy + \int_0^a \int_0^b X_m \frac{\partial^4 Y_n}{\partial y^4} X_m Y_n dx dy \right) \right] \\
 M_{12} &= M_{21} = 0
 \end{aligned}$$

References

1. Koizumi, M. FGM activities in Japan. *Compos. Part B Eng.* **1997**, *28*, 1–4. [CrossRef]
2. Jha, D.; Kant, T.; Singh, R. A critical review of recent research on functionally graded plates. *Compos. Struct.* **2013**, *96*, 833–849. [CrossRef]
3. Thanh, C.L.; Nguyen, T.N.; Vu, T.H.; Khatir, S.; Abdel Wahab, M. A geometrically nonlinear size-dependent hypothesis for porous functionally graded micro-plate. *Eng. Comput.* **2020**, *38*, 449–460. [CrossRef]
4. Cuong-Le, T.; Nguyen, K.D.; Nguyen-Trong, N.; Khatir, S.; Nguyen-Xuan, H.; Abdel-Wahab, M. A three-dimensional solution for free vibration and buckling of annular plate, conical, cylinder and cylindrical shell of FG porous-cellular materials using IGA. *Compos. Struct.* **2021**, *259*, 113216. [CrossRef]

5. Sahmani, S.; Fattahi, A.M.; Ahmed, N. Analytical treatment on the nonlocal strain gradient vibrational response of postbuckled functionally graded porous micro-/nanoplates reinforced with GPL. *Eng. Comput.* **2020**, *36*, 1559–1578. [[CrossRef](#)]
6. Zur, K.K.; Arefi, M.; Kim, J.; Reddy, J.N. Free vibration and buckling analyses of magneto-electro-elastic FGM nanoplates based on nonlocal modified higher-order sinusoidal shear deformation theory. *Compos. Part B Eng.* **2020**, *182*, 107601. [[CrossRef](#)]
7. Lü, C.; Lim, C.W.; Chen, W. Semi-analytical analysis for multi-directional functionally graded plates: 3-D elasticity solutions. *Int. J. Numer. Methods Eng.* **2009**, *79*, 25–44. [[CrossRef](#)]
8. Nemat-Alla, M. Reduction of thermal stresses by composition optimization of two-dimensional functionally graded materials. *Acta Mech.* **2009**, *208*, 147–161. [[CrossRef](#)]
9. Rad, A.B. Static analysis of two directional functionally graded circular plate under combined axisymmetric boundary conditions. *Int. J. Eng. Appl. Sci.* **2012**, *4*, 36–48.
10. Behravan Rad, A.; Alibeigloo, A. Semi-Analytical Solution for the Static Analysis of 2D Functionally Graded Solid and Annular Circular Plates Resting on Elastic Foundation. *Mech. Adv. Mater. Struct.* **2013**, *20*, 515–528. [[CrossRef](#)]
11. Nazari, H.; Babaei, M.; Kiarasi, F.; Asemi, K. Geometrically nonlinear dynamic analysis of functionally graded material plate excited by a moving load applying first-order shear deformation theory via generalized differential quadrature method. *SN Appl. Sci.* **2021**, *3*, 847. [[CrossRef](#)]
12. Khakpour, M.; Bazargan-Lari, Y.; Zahedinejad, P.; Kazemzadeh-Parsi, M.-J. Vibrations evaluation of functionally graded porous beams in thermal surroundings by generalized differential quadrature method. *Shock. Vib.* **2022**, *2022*, 8516971. [[CrossRef](#)]
13. Tornabene, F.; Fantuzzi, N.; Baccocchi, M.; Viola, E.; Reddy, J.N. A numerical investigation on the natural frequencies of FGM sandwich shells with variable thickness by the local generalized differential quadrature method. *Appl. Sci.* **2017**, *7*, 131. [[CrossRef](#)]
14. Shariyat, M.; Jafari, R. Nonlinear low-velocity impact response analysis of a radially preloaded two-directional-functionally graded circular plate: A refined contact stiffness approach. *Compos. Part B Eng.* **2013**, *45*, 981–994. [[CrossRef](#)]
15. Adineh, M.; Kadkhodayan, M. Three-dimensional thermo-elastic analysis of multi-directional functionally graded rectangular plates on elastic foundation. *Acta Mech.* **2017**, *228*, 881–899. [[CrossRef](#)]
16. Esmaeilzadeh, M.; Kadkhodayan, M. Dynamic analysis of stiffened bi-directional functionally graded plates with porosities under a moving load by dynamic relaxation method with kinetic damping. *Aerosp. Sci. Technol.* **2019**, *93*, 105333. [[CrossRef](#)]
17. Alipour, M.; Shariyat, M.; Shaban, M. A semi-analytical solution for free vibration of variable thickness two-directional-functionally graded plates on elastic foundations. *Int. J. Mech. Mater. Des.* **2010**, *6*, 293–304. [[CrossRef](#)]
18. Mikola, M.; Majak, J.; Pohlak, M.; Shvartsman, B. Higher order Haar wavelet method for vibration analysis of functionally graded beam. *AIP Conf. Proc.* **2022**, *2425*, 380003.
19. Majak, J.; Shvartsman, B.; Ratas, M.; Bassir, D.; Pohlak, M.; Karjust, K.; Eerme, M. Higher-order Haar wavelet method for vibration analysis of nanobeams. *Mater. Today Commun.* **2020**, *25*, 101290. [[CrossRef](#)]
20. Yas, M.; Moloudi, N. Three-dimensional free vibration analysis of multi-directional functionally graded piezoelectric annular plates on elastic foundations via state space based differential quadrature method. *Appl. Math. Mech.* **2015**, *36*, 439–464. [[CrossRef](#)]
21. Lieu, Q.X.; Lee, S.; Kang, J.; Lee, J. Bending and free vibration analyses of in-plane bi-directional functionally graded plates with variable thickness using isogeometric analysis. *Compos. Struct.* **2018**, *192*, 434–451. [[CrossRef](#)]
22. Lal, R.; Ahlawat, N. Buckling and vibrations of two-directional functionally graded circular plates subjected to hydrostatic in-plane force. *J. Vib. Control.* **2017**, *23*, 2111–2127. [[CrossRef](#)]
23. Sorrenti, M.; Di Sciuva, M.; Majak, J.; Auriemma, F. Static response and buckling loads of multilayered composite beams using the refined zigzag theory and higher-order Haar wavelet method. *Mech. Compos. Mater.* **2021**, *57*, 1–18. [[CrossRef](#)]
24. Majak, J.; Mikola, M.; Pohlak, M.; Eerme, M.; Karunanidhi, R. Modelling FGM materials. An accurate function approximation algorithms. *IOP Conf. Ser. Mater. Sci. Eng.* **2021**, *1140*, 012013. [[CrossRef](#)]
25. Niknam, H.; Akbarzadeh, A.; Rodrigue, D.; Therriault, D. Architected multi-directional functionally graded cellular plates. *Mater. Des.* **2018**, *148*, 188–202. [[CrossRef](#)]
26. Nguyen-Ngoc, H.; Cuong-Le, T.; Nguyen, K.D.; Nguyen-Xuan, H.; Abdel-Wahab, M. Three-dimensional polyhedral finite element method for the analysis of multi-directional functionally graded solid shells. *Compos. Struct.* **2023**, *305*, 116538. [[CrossRef](#)]
27. Asgari, M.; Akhlaghi, M. Natural frequency analysis of 2D-FGM thick hollow cylinder based on three-dimensional elasticity equations. *Eur. J. Mech.-A/Solids* **2011**, *30*, 72–81. [[CrossRef](#)]
28. Zafarmand, H.; Salehi, M.; Asemi, K. Three dimensional free vibration and transient analysis of two directional functionally graded thick cylindrical panels under impact loading. *Lat. Am. J. Solids Struct.* **2015**, *12*, 205–225. [[CrossRef](#)]
29. Yamanouchi, M.; Koizumi, M.; Hirai, T.; Shiota, I. FGM'90. In Proceedings of the First International Symposium on Functionally Gradient Materials, Sendai, Japan, 8–9 October 1990.
30. Shah, A.G.; Mahmood, T.; Naeem, M.N. Vibrations of FGM thin cylindrical shells with exponential volume fraction law. *Appl. Math. Mech.* **2009**, *30*, 607–615. [[CrossRef](#)]
31. Chi, S.-H.; Chung, Y.-L. Mechanical behavior of functionally graded material plates under transverse load—Part I: Analysis. *Int. J. Solids Struct.* **2006**, *43*, 3657–3674. [[CrossRef](#)]
32. Tornabene, F.; Viola, E. Free vibrations of four-parameter functionally graded parabolic panels and shells of revolution. *Eur. J. Mech. A/Solids* **2009**, *28*, 991–1013. [[CrossRef](#)]
33. Ghamkhar, M.; Naeem, M.N.; Imran, M.; Soutis, C. Vibration analysis of a three-layered FGM cylindrical shell including the effect of ring support. *Open Phys.* **2019**, *17*, 587–600. [[CrossRef](#)]

34. Pan, E. Exact solution for functionally graded anisotropic elastic composite laminates. *J. Compos. Mater.* **2003**, *37*, 1903–1920. [[CrossRef](#)]
35. Daikh, A.-A.; Belarbi, M.-O.; Ahmed, D.; Houari, M.S.A.; Avcar, M.; Tounsi, A.; Eltaher, M.A. Static analysis of functionally graded plate structures resting on variable elastic foundation under various boundary conditions. *Acta Mech.* **2023**, *234*, 775–806. [[CrossRef](#)]
36. Mourad, A.-H.I.; Almomani, A.; Sheikh, I.A.; Elsheikh, A.H. Failure analysis of gas and wind turbine blades: A review. *Eng. Fail. Anal.* **2023**, *146*, 107107. [[CrossRef](#)]
37. Matsunaga, H. Free vibration and stability of functionally graded shallow shells according to a 2D higher-order deformation theory. *Compos. Struct.* **2008**, *84*, 132–146. [[CrossRef](#)]
38. Lim, C.; Zhang, G.; Reddy, J. A higher-order nonlocal elasticity and strain gradient theory and its applications in wave propagation. *J. Mech. Phys. Solids* **2015**, *78*, 298–313. [[CrossRef](#)]
39. Eringen, A.C. Plane waves in nonlocal micropolar elasticity. *Int. J. Eng. Sci.* **1984**, *22*, 1113–1121. [[CrossRef](#)]
40. Daikh, A.A.; Houari, M.S.A.; Belarbi, M.O.; Mohamed, S.A.; Eltaher, M.A. Static and dynamic stability responses of multilayer functionally graded carbon nanotubes reinforced composite nanoplates via quasi 3D nonlocal strain gradient theory. *Def. Technol.* **2022**, *18*, 1778–1809. [[CrossRef](#)]
41. Basha, M.; Daikh, A.A.; Melaibari, A.; Wagih, A.; Othman, R.; Almitani, K.H.; Hamed, M.A.; Abdelrahman, A.; Eltaher, M.A. Nonlocal strain gradient theory for buckling and bending of FG-GRNC laminated sandwich plates. *Steel Compos. Struct.* **2022**, *43*, 639–660.
42. Ghandourah, E.E.; Daikh, A.A.; Alhawsawi, A.M.; Fallatah, O.A.; Eltaher, M.A. Bending and buckling of FG-GRNC laminated plates via quasi-3D nonlocal strain gradient theory. *Mathematics* **2022**, *10*, 1321. [[CrossRef](#)]
43. Melaibari, A.; Daikh, A.A.; Basha, M.; Abdalla, A.W.; Othman, R.; Almitani, K.H.; Hamed, M.A.; Abdelrahman, A.; Eltaher, M.A. Free vibration of FG-CNTRCs nano-plates/shells with temperature-dependent properties. *Mathematics* **2022**, *10*, 583. [[CrossRef](#)]
44. Alazwari, M.A.; Daikh, A.A.; Eltaher, M.A. Novel quasi 3D theory for mechanical responses of FG-CNTs reinforced composite nanoplates. *Adv. Nano Res.* **2022**, *12*, 117–137.
45. Alijani, F.; Amabili, M.; Karagiozis, K.; Bakhtiari-Nejad, F. Nonlinear vibrations of functionally graded doubly curved shallow shells. *J. Sound Vib.* **2011**, *330*, 1432–1454. [[CrossRef](#)]
46. Chorfi, S.; Houmat, A. Non-linear free vibration of a functionally graded doubly-curved shallow shell of elliptical plan-form. *Compos. Struct.* **2010**, *92*, 2573–2581. [[CrossRef](#)]
47. Trinh, M.-C.; Kim, S.-E. A three variable refined shear deformation theory for porous functionally graded doubly curved shell analysis. *Aerosp. Sci. Technol.* **2019**, *94*, 105356. [[CrossRef](#)]

**Disclaimer/Publisher’s Note:** The statements, opinions and data contained in all publications are solely those of the individual author(s) and contributor(s) and not of MDPI and/or the editor(s). MDPI and/or the editor(s) disclaim responsibility for any injury to people or property resulting from any ideas, methods, instructions or products referred to in the content.